

Report Title: Examination of cable joints from Penrose Substation

Authors: Bob Dean and Stephen Pitman

Client: Vector Ltd and Transpower NZ Ltd

Client Reference: 4500281283

Report Number: 2015-0356

Project Number: EDP2744001

Report Version: Final Report

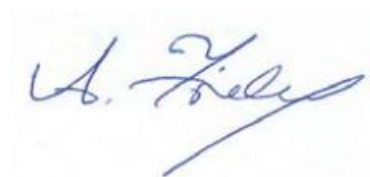
Document Control: Privileged and Confidential

Report Checked by:

A handwritten signature in blue ink, appearing to read "J. Stubbs".

Joe Stubbs
Electrical Engineer

Approved by:

A handwritten signature in blue ink, appearing to read "A. Friday".

Alan Friday
Head of Engineering Design Performance

November 2015

Ref. EDP2744001/Edif ERA Report 2015-0356 Final.docx

PURPOSE OF DISTRIBUTION:

This document is distributed to Vector Ltd and Transpower NZ Ltd for the sole purpose of obtaining legal advice. Rights to copy or distribute this document are only granted for the stated purpose. Edif ERA hereby gives permission for the above named clients to reproduce (the waiving of privilege being at the clients' discretion) this report in its entirety and without alteration and to distribute it as required in connection with the specific investigation.

© ERA Technology Limited 2015
All Rights Reserved
No part of this document may be copied or otherwise reproduced without the prior written permission of ERA Technology Limited. If received electronically, recipient is permitted to make such copies as are necessary to: view the document on a computer system; comply with a reasonable corporate computer data protection and back-up policy and produce one paper copy for personal use.

Distribution List

Client	(1)
Project File	(1)
Information Centre	(1)

DOCUMENT CONTROL

Distribution of this document by the recipient(s) is authorised in accordance with the following commercial restrictive markings:

Commercial-in-confidence : No distribution or disclosure outside of the recipient's organisation is permitted without the prior written permission of Edif ERA.

Distributed-in-confidence : Distribution of the document shall be in accordance with the document distribution list and no further distribution or disclosure shall be allowed without the prior written permission of Edif ERA.

Recipient-in-confidence : Edif ERA distributes this document to the recipient on the condition that no further distribution or disclosure by the recipient shall be allowed.

Where specified the document may only be used in accordance with the 'Purpose of Distribution' notice displayed on the cover page.

For the purpose of these conditions, the recipient's organisation shall not include parent or subsidiary organisations.

Permission to disclose within recipient's organisation does not extend to allowing access to the document via Internet, Intranet or other web-based computer systems.

Commercial restrictive markings are as contained in page header blocks.

If no restrictive markings are shown, the document may be distributed freely in whole, without alteration, subject to Copyright.

Edif ERA
Cleeve Road
Leatherhead
Surrey KT22 7SA, England
Tel : +44 (0) 1372 367350
Fax: +44 (0) 1372 367359

Read more about Edif ERA on our Internet page at: www.edifgroup.com

Summary

This report was prepared as a supporting document for the joint Transpower/Vector investigation into the fire that occurred in a cable trench at Transpower's Penrose Substation on Sunday 5th October 2014. The report describes the results of examinations of cable joints removed from the cable trench which were examined at Edif ERA's laboratory in the UK.

In addition to the examination of the cable joints, Edif ERA also examined and tested samples of cables and other materials removed from the trench. This work is covered in a separate report, Edif ERA Report Reference 2015-0027, Ref. 1, the conclusions of which were that the XLPE, Oil Filled and PILC cables were all in good condition for their age. A number of adverse observations were recorded, but all of these were minor in nature. Based on the results obtained the residual life of the XLPE, OF and PILC cables was predicted to be 20, 15 and 10 years respectively.

From the examination of the cable joints detailed in this report it was concluded that:

- Based on the timings of the cable faults that were recorded, the position of the fault, its appearance and from past experience, the PILC/XLPE transition joint fault in the 11kV Remuera K10 circuit was the original fault and not a result of the fire.
- From the profile of the eroded area, the fault position and from previous experience, the PILC/XLPE transition joint fault started in the PILC cable crutch and the arc propagated preferentially away from the cable crutch towards the centre of the joint.
- A black feature/stain indicative of deterioration or possibly incipient electrical distress was present on the PILC core paper tape insulation of the unfailed PILC to XLPE transition joint below the lead sheath and in the vicinity of the lead cut. Components of the yellow void filling mastic were present in the feature.
- From Edif ERA's previous experience of examining failed PILC cable joints, the PILC cable crutch is a weak area where failures are likely to occur in heat shrink joints on aged belted PILC cables.
- The bimetallic ferrules from the PILC to XLPE transition joints were found to have been sound. The parting of the bimetallic interface was found to be a consequence of the fire. The compression ferrules were found to have been sound.
- A portion of nut was found to be present on the top wall stud of the collapsed cable support frame, thus confirming that the frame had been assembled correctly. The evidence suggests the nuts found on the floor of the cable trench at 69.5m, the position of the collapsed cable support, were not in place on the studs at the time of the fire. The evidence indicates the nuts had not been associated with the frame.

- The PILC cables had severely corroded steel tape armour but this would not have affected the life of the cables.
- The PILC cable cast iron joint shells were corroded and had slight bitumen leaks but this would not have affected the life of the cast iron joints because they have an inner bitumen filled lead sleeve.
- There was a sharp point on one strand of the PILC cable in the PN60 cast iron cable joint. This could have developed into a breakdown fault in perhaps 5 to 10 years (a very rough estimate).
- The five XLPE straight joints examined were generally found to be in sound condition. In one joint one of the two compression ferrules connecting the cable earth return conductors had not satisfactorily gripped the conductor wires.
- There were no other incipient faults in any of the joints sent to ERA for examination.

From Edif ERA's experience of examining failed PILC cable joints, the PILC cable crutch is a weak area where failures are likely to occur in heat shrink joints on aged belted PILC cables. The aged PILC cable, heat shrink joint failures examined previously by Edif ERA have in most cases been attributed to damage to the aged, relatively fragile, paper insulation which had been caused during the jointing process when the cores were being manipulated.

Contents

	Page No.
1. Introduction	13
2. Failed Heat Shrink PILC to XLPE Transition Joint 3-B-0, PN33	13
3. Unfailed 11kV Remuera K10 PILC/XLPE transition joint 3-B-0, PN53	28
3.1 Joint strip down	28
3.2 Resistance measurements	32
3.3 Microscopy on PILC cable components	33
3.4 Tensile testing	41
3.5 Examination and testing of bimetallic welds	42
3.6 Further analysis of crimps on PN33 and PN53 connectors	50
4. Examination of nuts and studs from cable trench	56
5. Possible causes of failure of heat shrink transition joint 3-B-0, PN33	70
5.1 Unlikely causes of failure	70
5.2 Moisture ingress and effect of load changes	70
5.3 Past experience	71
5.4 Position of fault within the 3BO failed transition joint, PN53	71
5.5 Position of transition joint within the trench	72
5.6 Timing of joint failure	72
6. Condition of other cable joints	73
6.1 11kV cast iron joint PN57 3DO, 50m	73
6.2 11kV cast iron joint 3BO, PN60	77
6.3 Cast iron joint PN28, 3A0, 71 – 75m	80

6.4	33kV XLPE 800/400mm ² transition joint, 1DY, 5m	84
6.5	33kV 630/400mm ² XLPE insulated transition joint, 03 NWMT YØ 1B- PN59	86
6.6	XLPE single core transition joint, Remuera No. 2, 1DZ, PN55	87
6.7	XLPE transition joint Newmarket 03 Red Phase, PN58	89
6.7.1	33kV XLPE 800/400mm ² transition joint, PN 56, 1AX, 5m	91
7.	Conclusions	95
8.	References	96

Tables List

	Page No.
Table 1: Conductivity measurements on bimetallic connectors from PN53	33
Table 2: Tensile tests on bi-metallic connectors from PN53	42
Table 3: Transverse tests on bi-metallic weld on PN 53 connector.....	49
Table 4: Degree of achieved compression measurement at depression	50
Table 5: Degree of achieved compression measurement at non-depression.....	51
Table 7: Fault times, position, duration and arc crater volume.....	72

Figures List

	Page No.
Figure 1: Failed transition joint from 3-B-0.....	13
Figure 2: Distance to fault measured from friction weld on ferrule.....	14
Figure 3: Fault area after cleaning conductors and clamping in position with binder wires.....	14
Figure 4: Arc eroded end of green labelled core on cable side of fault.....	15
Figure 5: Position of fault on failed joint highlighted on un-failed transition joint	15
Figure 6: P1070015 from examination in New Zealand.....	16
Figure 7: P1070019 from examination in New Zealand (brightness and contrast altered).....	16
Figure 8: Faulted transition joint with core papers still present on cable side of fault.....	17
Figure 9: Closer view of core papers on faulted transition joint	17
Figure 10: Parted bi-metallic ferrules on failed joint	18
Figure 11: Aluminium side of bi-metallic connectors	18
Figure 12: Aluminium weld surface from white taped core	19

Figure 13: Copper side of bi-metallic connectors	19
Figure 14: Side view showing material adhering to copper side of white taped connector	20
Figure 15: Sections through copper & aluminium ferrules, white phase connector.....	27
Figure 16: Section through aluminium ferrule, green phase connector	27
Figure 17: Central insulating sleeve from un-failed joint.....	28
Figure 18: End of insulation sleeve shown in Figure 15.....	28
Figure 19: Dark surface on core 2 beneath belt papers and lead sheath	29
Figure 20: Section of discoloured core identification paper from core 2	30
Figure 21: Three cores of PILC cable with localised discolouration on core 2.....	31
Figure 22: Localised "blotches" on conductor strands on core 1	31
Figure 23: Localised apparent thermal effect on conductor, core 3	32
Figure 24: Bimetallic connectors after removing insulation.....	32
Figure 25: Discoloured conductor strand prior to SEM analysis.....	34
Figure 26: Identification paper from core 2, un-failed transition joint.....	39
Figure 27: Stained paper with section cut out for SEM analysis.....	39
Figure 28: SEM image of paper in relatively good condition	40
Figure 29: SEM image of fractured edge of degraded paper.....	41
Figure 30: Tensile test on red phase bimetallic connector from PN53.....	42
Figure 31: Red connector aluminium/copper interface (scale approx. 1mm from top to bottom)	43
Figure 32: Initial arrangement for testing bi-metallic weld on PN 53 connector	47
Figure 33: Initial loading arrangement.....	48
Figure 34: Weld interface surfaces showing aluminium adhering to copper surface	48
Figure 35: Half of connector from PN53 mounted in oven	49

Figure 36: Half of connector from PN53 after 15 minutes at 600°C.....	50
Figure 37: PN 33 (failed joint) Good compaction on Red Al, crimped section	52
Figure 38: PN 33 (failed joint) Good compaction on Red Cu, crimped section	52
Figure 39: PN 33 (failed joint) Good compaction on white Al, crimped section	53
Figure 40: PN 33 (failed joint) Good compaction on white Cu, crimped section	53
Figure 41: PN 53 white, copper, crimped section.....	54
Figure 42: PN 33 green, copper, crimped section.....	54
Figure 43: PN53 Green connector with good conductor insertion and compaction.....	55
Figure 44: PN53 Red connector with good conductor insertion and compaction	55
Figure 45: PN53 White connector with conductor strands fully inserted into ferrules	55
Figure 46: PN64 top bolt 69.5m (Failed Support Position)	56
Figure 47: PN65 bottom bolt 69.5m (Failed Support Position).....	56
Figure 48: PN66 two nuts 69.5m (Failed Support Position).....	57
Figure 49: PN67 bottom stud and nut 69m	57
Figure 50: PN68 top stud and nut 69m	57
Figure 51: PN67 Nut surface	58
Figure 52: PN67 Thread surface.....	59
Figure 53: Damage to galvanised layer due to temperatures above 250-350°C.....	60
Figure 54: PN64 SEM images and chemical analysis.....	61
Figure 55: PN64 nut microstructure	62
Figure 56: PN64 nut SEM image and bulk composition.....	63
Figure 57: PN64 and PN65 microstructure	64
Figure 58: Higher magnification views of PN64 and PN65 pearlite microstructure	65

Figure 59: Surface nodule on Stud PN64 indicative of arcing and localised melting of	66
Figure 60: Surface corrosion on PN66 nut screw-threads	66
Figure 61: PN66 nut cross section and SEM analysis	67
Figure 62: PN66 nut cross section microstructure.....	68
Figure 63: PN66 SEM cross section and material analysis	69
Figure 64: PN66 nut surface, SEM image and analysis	70
Figure 65: Corroded joint shell, PN57	74
Figure 66: Severely corroded joint shell retaining bolt, PN57	74
Figure 67: Corroded steel tape armour, PN57	75
Figure 68: S shaped profile of cores within joint shell and kink at switchroom end, PN57.....	75
Figure 69: Conductor partly pulled out of ferrule.....	76
Figure 70: Cable fault position on Gavin St side of joint, PN57	77
Figure 71: Fault position after removing armour, PN57	77
Figure 72: Abraded appearance of conductor strands on Gavin Street side of joint, PN57.....	77
Figure 73: Eroded bolt on cast iron joint shell, PN60	78
Figure 74: PILC cable joint after removing joint shell, inner lead sleeve and bitumen, PN60.....	78
Figure 75: Sharp protrusion from PILC conductor strand, PN60	79
Figure 76: Dark stain on conductor beneath hole in core papers, PN60.....	79
Figure 77: Corroded bolt on cast iron joint shell, PN28.....	80
Figure 78: Degraded belt papers, PN28	80
Figure 79: Central taped insulation over ferrule PN28	81
Figure 80: Core 1 ferrule, PN28.....	81
Figure 81: Dent in lead sheath, PN28.....	82

Figure 82: Bend at temporary spreader position and penetration of lead solder, PN28	82
Figure 83: Split in insulation paper at butt gap position, PN28	83
Figure 84: Gap visible between conductor and bore of ferrule.....	83
Figure 85: 33kV XLPE s/c joint after removing outer HS tube and earth screen, PN54.....	84
Figure 86: Screen wires fell out of compression ferrule	84
Figure 87: XLPE joint after removing outer heat shrink and stress control tubes PN54	85
Figure 88: XLPE core on 400mm ² cable and ferrule coated with mastic, PN54	85
Figure 89: 400/630mm ² XLPE transition joint PN59	86
Figure 90: Screen wire connections across joint, PN59	86
Figure 91: Shear head bolt connector, PN59	87
Figure 92: Hot melt adhesive visible at end of WCSM outer tubing, PN55	87
Figure 93: Yellow mastic applied over ferrule and screen terminations, PN55	88
Figure 94: XLPE insulation and compression ferrule, PN55	88
Figure 95: XLPE transition joint after removing outer WCSM tube, PM58.....	89
Figure 96: End of cable sheath and remains of hot melt adhesive, PN58	89
Figure 97: Stress control tube over phase conductor ferrule and screen wires connection, PN58	90
Figure 98: XLPE insulation and compression ferrule, PN58	90
Figure 99: 33kV XLPE s/c joint after removing outer HS tube and earth screen, PN56.....	91
Figure 100: Ferrule connecting cable screen wires across the joint PN 56	92
Figure 101: yellow mastic showing void and ridge of aluminium ferrule PN 56	93
Figure 102: Screen termination features PN 56.....	93
Figure 103: Compression transition ferrule PN56	94

Abbreviations List

Al	:	Aluminium
CCI	:	Cable Consulting International Ltd
Cu	:	Copper
DOP	:	Degree of polymerisation
EDX	:	Energy Dispersive X-ray
FTIR	:	Fourier transform infrared spectroscopy
MIND	:	Mass impregnated non draining
OF	:	Oil filled
OI	:	Oxygen index
OIT	:	Oxidation induction time
Pb	:	Lead
PE	:	Polyethylene
PILC	:	Paper insulated lead covered
PVC	:	Polyvinyl chloride
Sb	:	Antimony
SEM	:	Scanning Electron Microscope
XLPE	:	Cross-linked polyethylene

1. Introduction

This report was prepared as a supporting document for the joint Transpower/Vector investigation into the fire that occurred in a cable trench at Transpower's Penrose Substation on Sunday 5th October 2014. There are a number of cable trenches and above ground cable racks at the Penrose Substation. The fire occurred in the cable trench that runs east-west across the 220 kV switchyard and all references to a cable trench in this document are to this particular trench.

Edif ERA examined and tested samples of cables and other materials removed from the trench. This work is covered in a separate report, Edif ERA Report Reference 2015-0027, Ref. 1, the conclusions of which were that the XLPE, oil filled and PILC cables were all in good condition for their age. A number of adverse observations were recorded, but all of these were minor in nature. Based on the results obtained the residual life of the XLPE, OF and PILC cables was predicted to be 20, 15 and 10 years respectively.

This report describes the results of examinations of cable joints removed from the cable trench carried out at Edif ERA's laboratory in the UK.

2. Failed Heat Shrink PILC to XLPE Transition Joint 3-B-0, PN33

The failed transition joint, PN33, had been partly examined before it was delivered to ERA.

Most of the heat-shrink material, XLPE core insulation and PILC cable insulation had been burnt away in the fault and subsequent fire, Figure 1. There was no evidence of any electrical breakdown on the XLPE side of the joint.



Figure 1: Failed transition joint from 3-B-0

The lead sheath had melted from the PILC cable. There was arc erosion on all 3 cores of the PILC cable but the erosion was most severe on the core wrapped with green PVC tape which had been cut through by the arc erosion. The approximate centre of the erosion was close to the PILC cable crutch and was measured to be 384mm from the copper side of the friction weld, Figure 2.

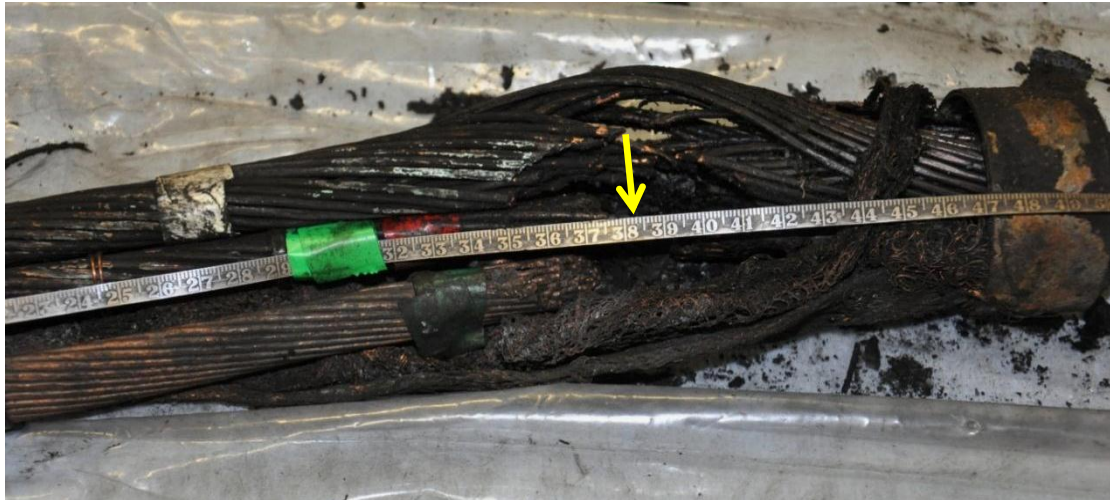


Figure 2: Distance to fault measured from friction weld on ferrule

The arc eroded end of the green labelled core on the cable side of the fault had been cut by the arc in a relatively straight line almost perpendicular to the axis of the cable, Figure 3 and Figure 4.



Figure 3: Fault area after cleaning conductors and clamping in position with binder wires



Figure 4: Arc eroded end of green labelled core on cable side of fault

The arc eroded area extended between 345mm and 425mm from the bi-metallic connector interface. From measurements on the unfaulted transition joint from the same circuit, if the two joints were made to the same dimensions, the straight arc eroded edge was at or close to the lead sheath cut back position and the centre of the arc eroded area was at or close to a point 5mm from the end of the translucent heat shrink tube, Figure 5.



Figure 5: Position of fault on failed joint highlighted on un-failed transition joint

From photographs P01070015 and P01070019, taken during the partial strip down in New Zealand, the remains of the core insulating tapes were still present on the cable side of the fault position right up to the edge of the fault eroded region, Figure 6 and Figure 7.



Figure 6: P1070015 from examination in New Zealand



Figure 7: P1070019 from examination in New Zealand (brightness and contrast altered)

These insulating tapes next to the fault position were still partly present when the sample was received at ERA, Figure 8 and Figure 9. They were very fragile and tended to fall away as the cable was manhandled.



Figure 8: Faulted transition joint with core papers still present on cable side of fault



Figure 9: Closer view of core papers on faulted transition joint

The bimetallic connector ferrules appeared to be correctly compressed onto the aluminium and copper conductors. The connectors had parted at the friction welds. The central insulators and core papers had burnt away or been removed on either side of the bi-metallic connectors, Figure 10.

There was little of the copper and aluminium material left adhering to the other side of the friction weld interfaces on the red and green taped cores. On the white taped core there was an indentation on the surface of the aluminium side and a raised area of what appeared to be aluminium on the copper side, Figure 11 to Figure 14.



Figure 10: Parted bi-metallic ferrules on failed joint



Figure 11: Aluminium side of bi-metallic connectors



Figure 12: Aluminium weld surface from white taped core



Figure 13: Copper side of bi-metallic connectors

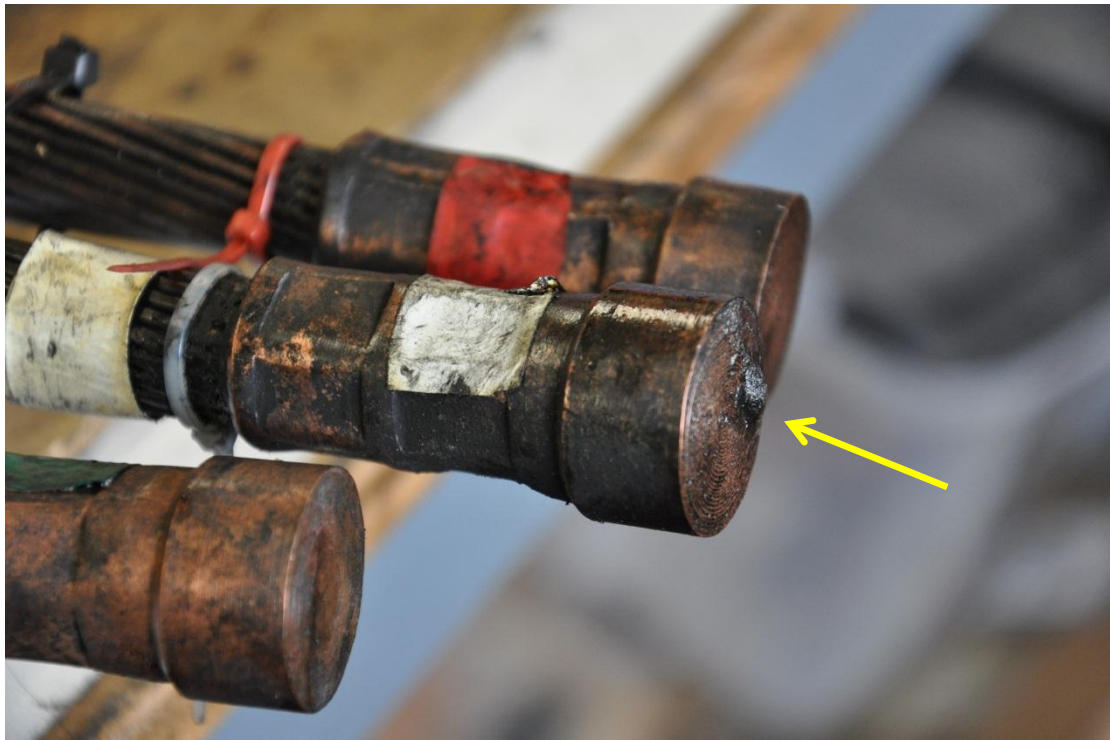


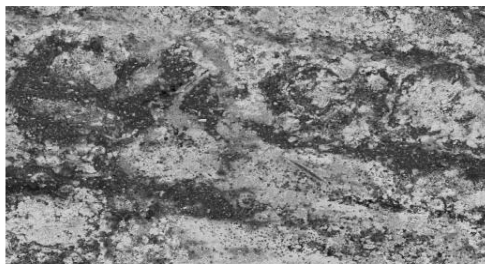
Figure 14: Side view showing material adhering to copper side of white taped connector

Bimetallic weld surfaces from the red labelled core on the failed joint were examined in the SEM. The results indicated that there was aluminium present on the copper surface and copper present on the aluminium surface, in both cases not uniformly across the surfaces but in localised areas. In these areas the quantities of copper to aluminium were in roughly stoichiometric proportions indicating that the copper and aluminium were molten in these areas at some point, presumably during the welding process.

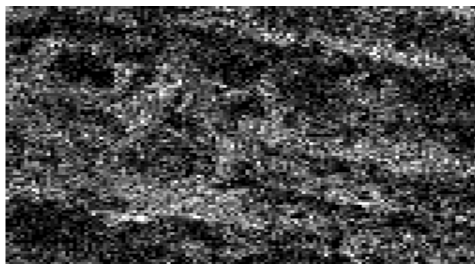
From the SEM EDX analysis, the raised area on the copper surface of the white labelled connector, indicated in Figure 14, contained copper and aluminium with combustion products, carbon and oxygen, together with small quantities of chlorine and iron.

There were localised lead deposits on both the copper and the aluminium bi-metallic weld surfaces. SEM images and EDX spectra are shown below:

EDP2744001 Penrose Fire



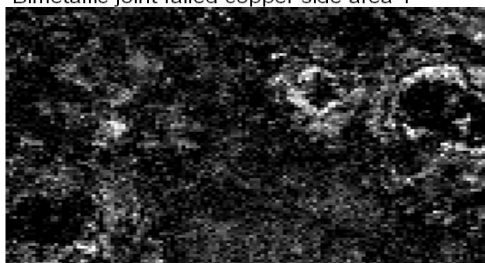
Bimetallic joint failed copper side area 1



C Ka1 2



O Ka1



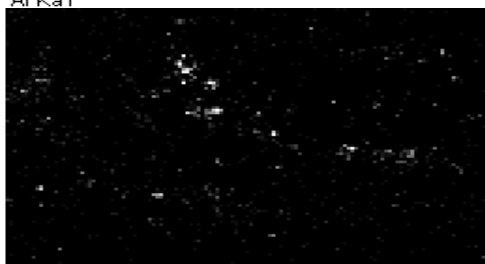
Al Ka1



S Ka1



Cl Ka1



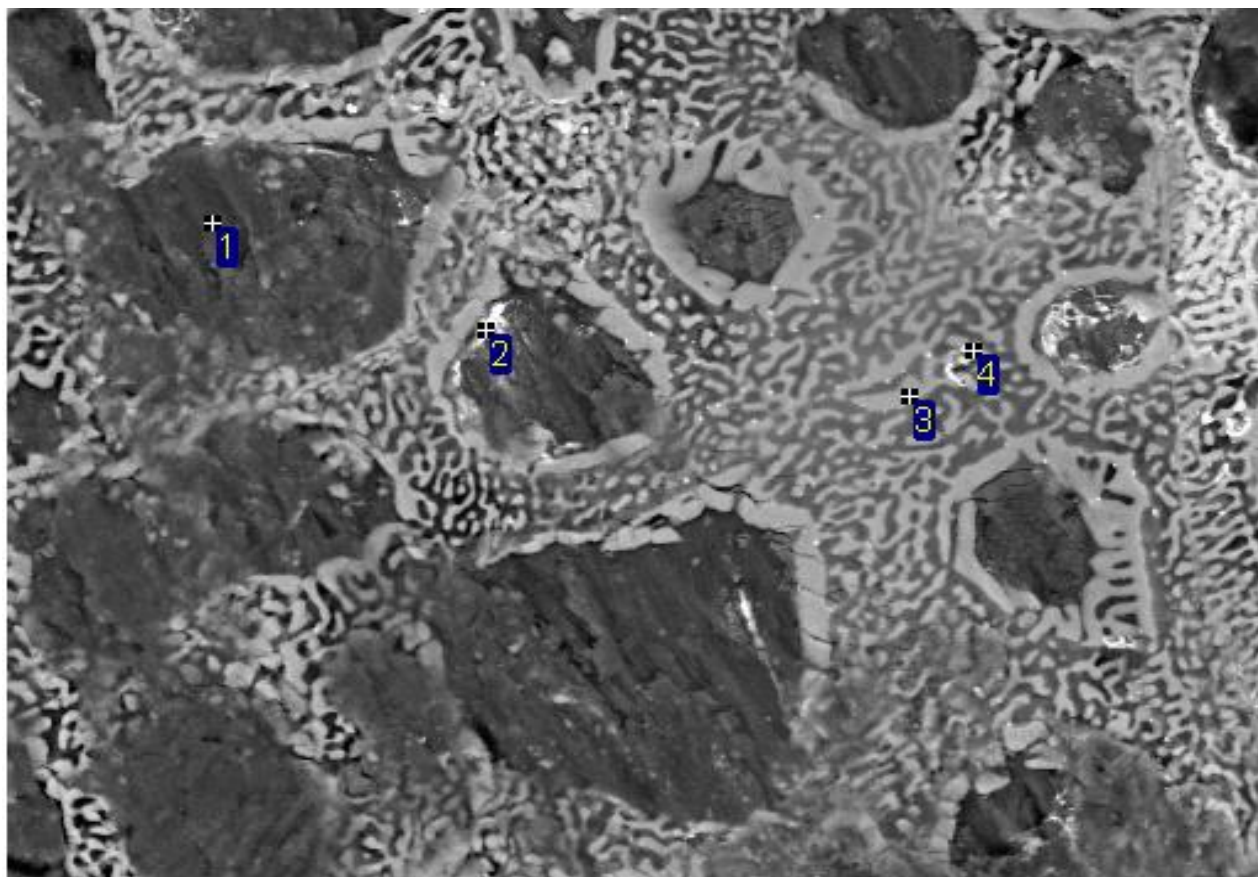
Fe Ka1



Cu Ka1

Comment: EDX mapping of copper weld surface in an area where there was aluminium present, shows deposition of aluminium, sulphur,

EDP2744001 Penrose Fire



70µm

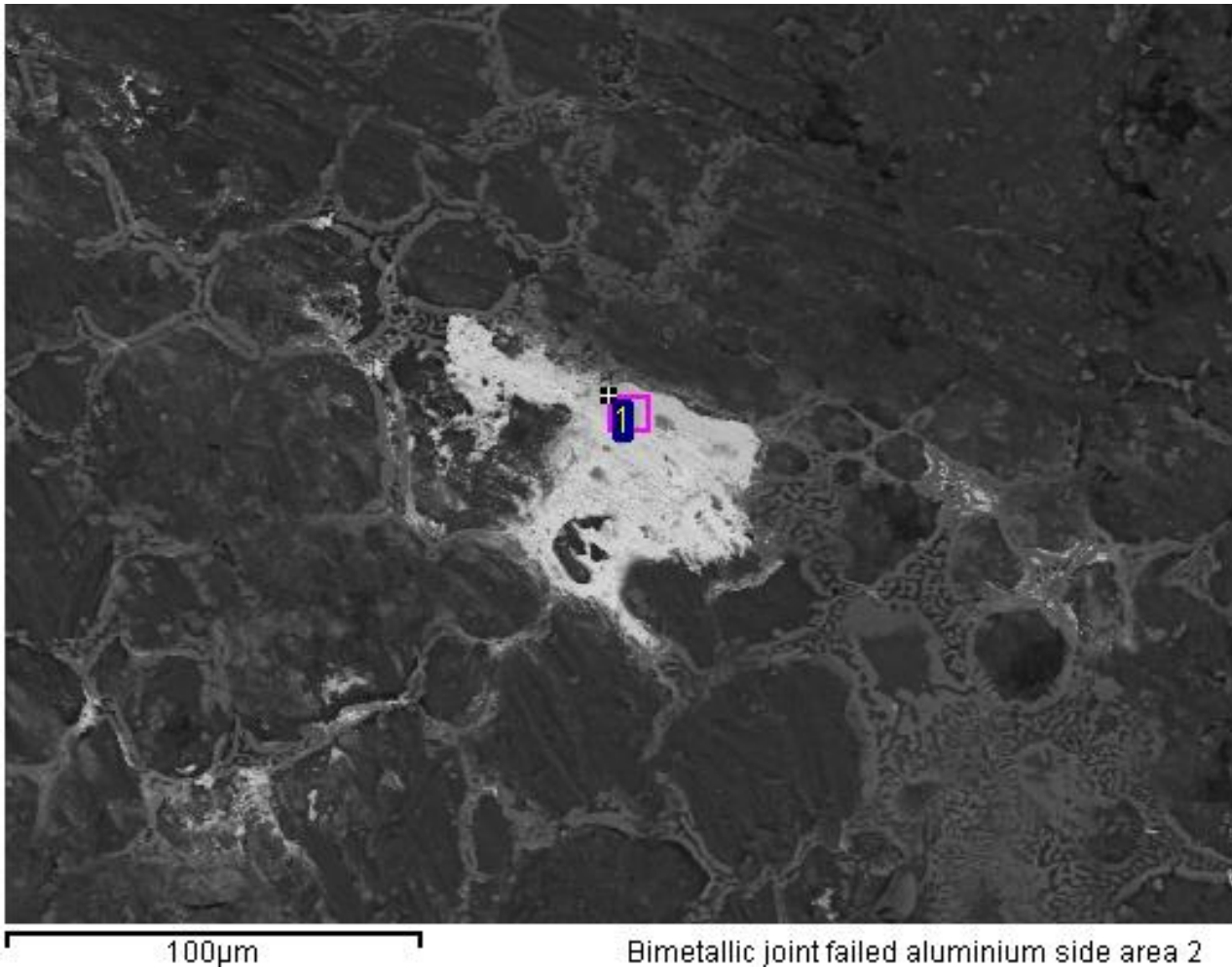
Bimetallic joint failed aluminium side area 1

Processing option: All elements analysed (normalised)

Spectrum	In stats.	C	O	Al	Fe	Cu	Pb	Total
1	Yes		2.3	94.4		3.3		100.0
2	Yes	9.1	15.0	40.2		7.2	28.6	100.0
3	Yes	4.2	2.0	49.9	3.0	40.9		100.0
4	Yes	20.6	13.0	15.6	1.0	33.3	16.5	100.0

All results in weight%. EDX spectrum indicates small quantities of lead on aluminium surface

EDP2744001 Penrose Fire

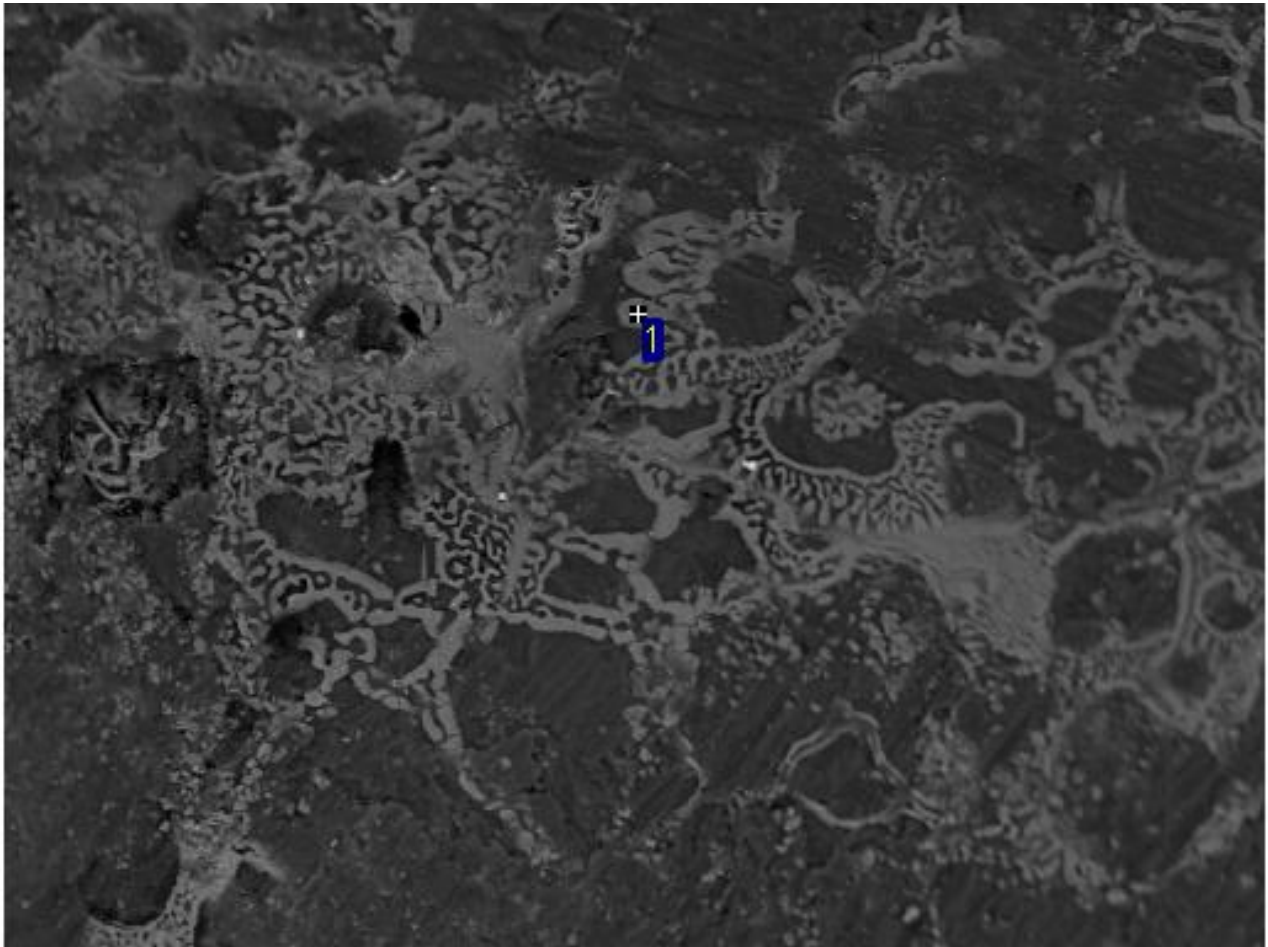


Processing option: All elements analysed (normalised)

Spectrum	In stats.	C	O	Al	Cu	Pb	Total
1	Yes	5.4	8.1	1.9	1.7	82.9	100.0

All results in weight%. EDX analysis indicated area of lead on aluminium surface

EDP2744001 Penrose Fire



100µm

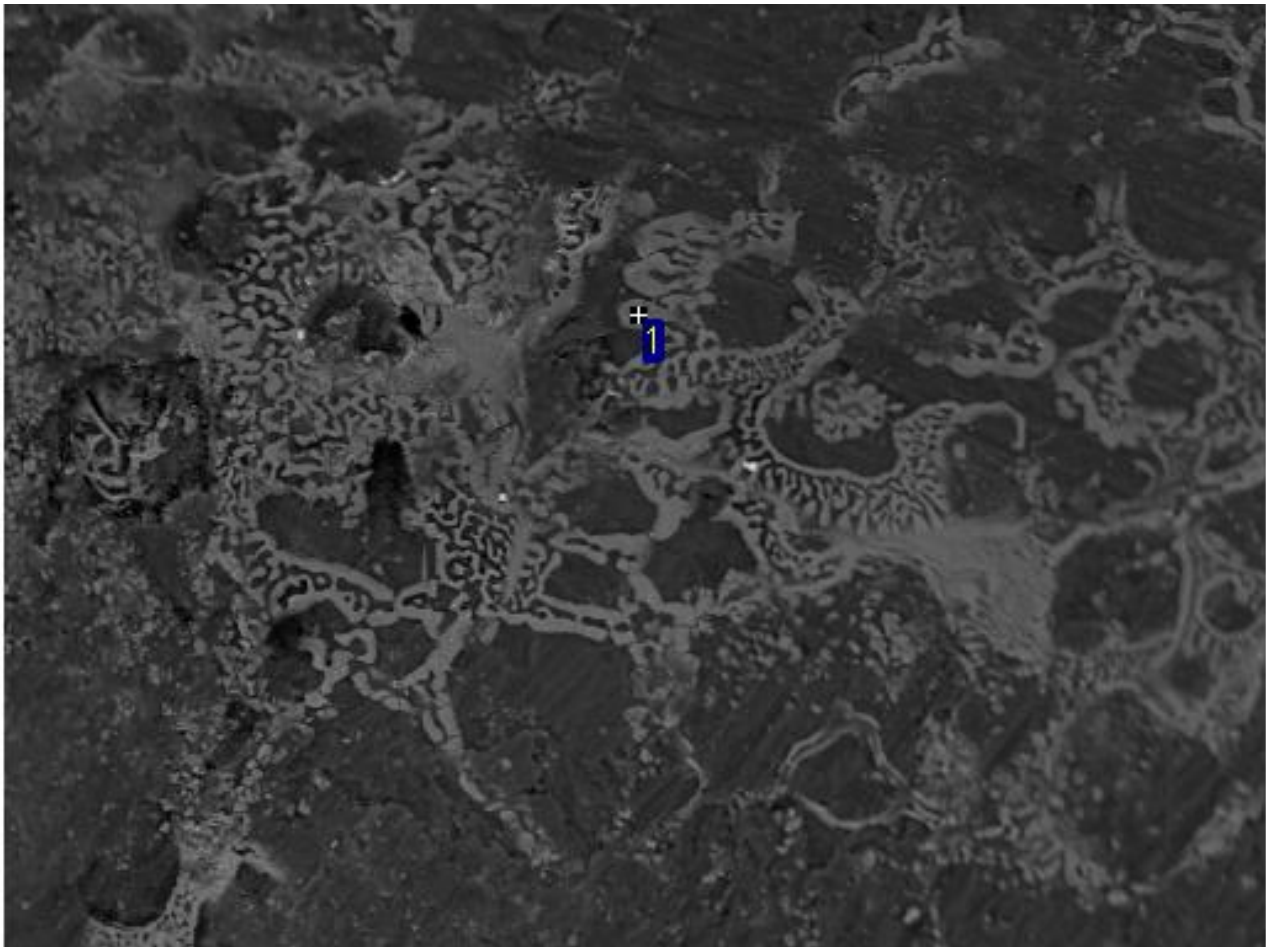
Bimetalllic joint failed aluminium side area 3

Processing option: All elements analysed (normalised)

Spectrum	In stats.	Al	Cu
1	Yes	76.7	23.3

All results in atomic%. EDX analysis indicates grey areas are a combination of aluminium and copper

EDP2744001 Penrose Fire



100µm

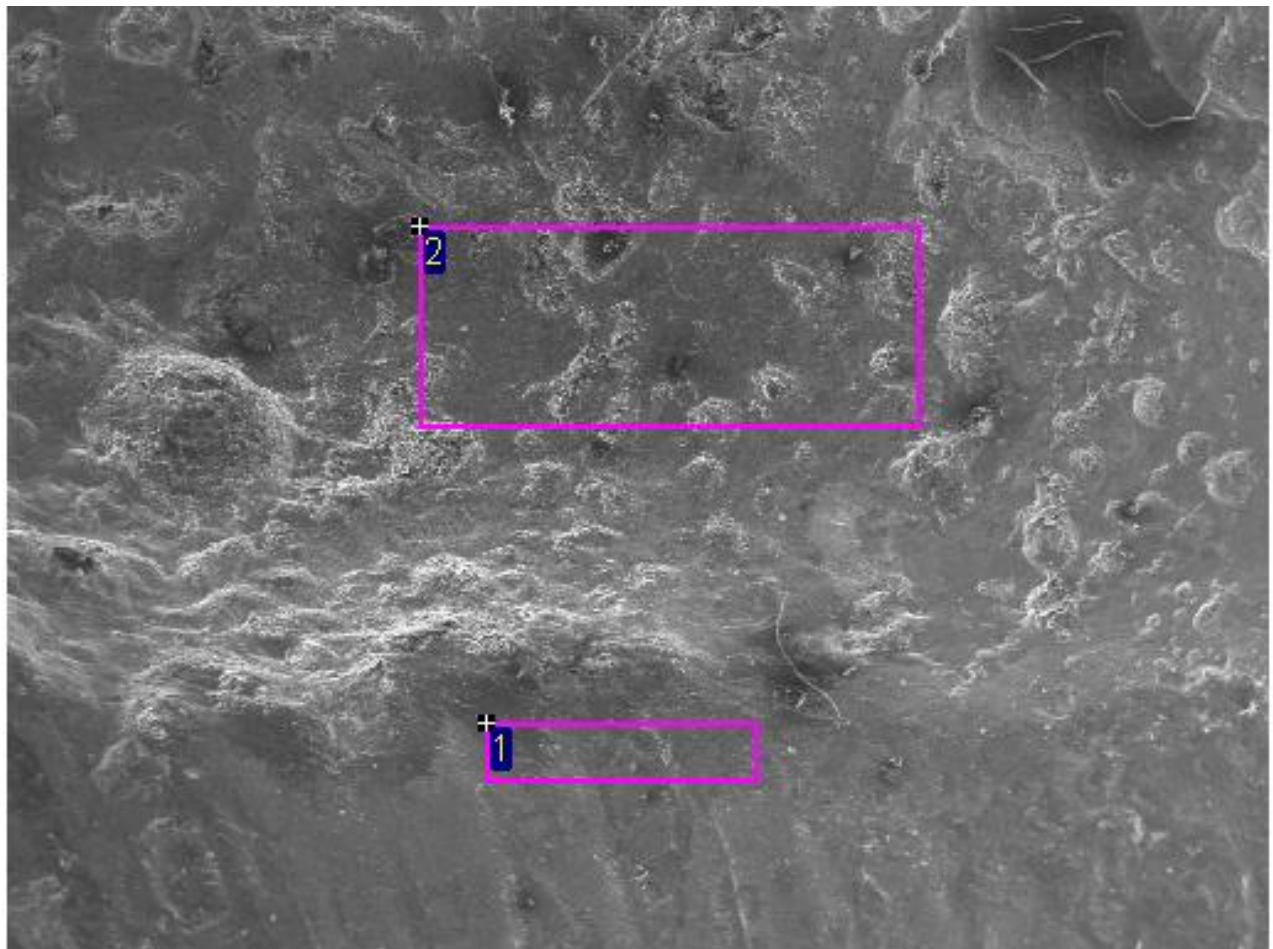
Bimetallic joint failed aluminium side area 3

Processing option: All elements analysed (normalised)

Spectrum	In stats.	Al	Cu	Total
1	Yes	58.29	41.71	100.00
CuAl2 stoichiometric	Yes	46.29	53.71	100.00

All results in weight%. EDX analysis indicates the grey area on the aluminium side the aluminium side of the bimetallic connector contained copper and aluminium at close to the stoichiometric ratio.

EDP2744001 Penrose Fire



2mm

Bimetallic joint failed copper side 2 area 1

Processing option: All elements analysed (normalised)

Spectrum	In stats.	C	O	Al	S	Cl	Fe	Cu	Total
1	Yes	49.1	17.0	8.3		1.2	1.3	23.0	100.0
2	Yes	41.7	19.9	13.1	0.3	1.3	1.7	22.0	100.0

All results in weight%. Spiral grooves in the copper can be seen in area 1. Area 2 is the area of raised grey material on the copper surface.

There were oxidation products present together with aluminium and copper and small quantities of chlorine and iron.

The aluminium and copper compression ferrules were cut longitudinally and transversely. All of the conductors had been inserted into the compression ferrules past the end of the final compression. The crimps had been applied uniformly over the combined thickness of stranded conductor and compression ferrule.

In Figure 15, the end of the stranded aluminium conductor was 2.7mm from the blind end of the bore of the aluminium ferrule and the end of the stranded copper conductor was 3mm from the blind end of the bore of the copper ferrule. In Figure 16, the end of the stranded aluminium conductor was 3mm from the blind end of the bore of the aluminium ferrule

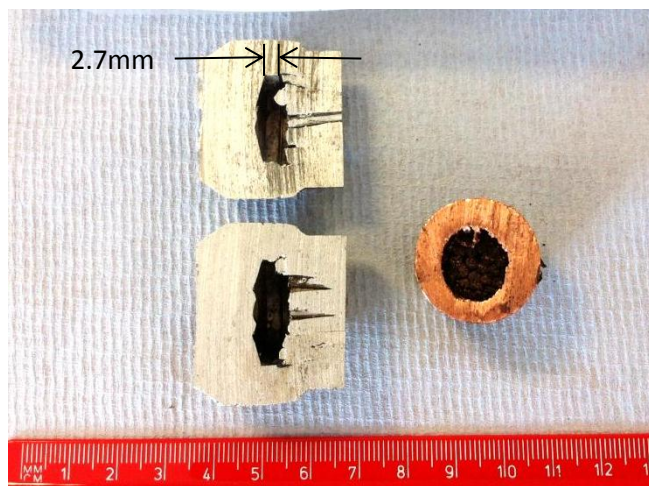


Figure 15: Sections through copper & aluminium ferrules, white phase connector

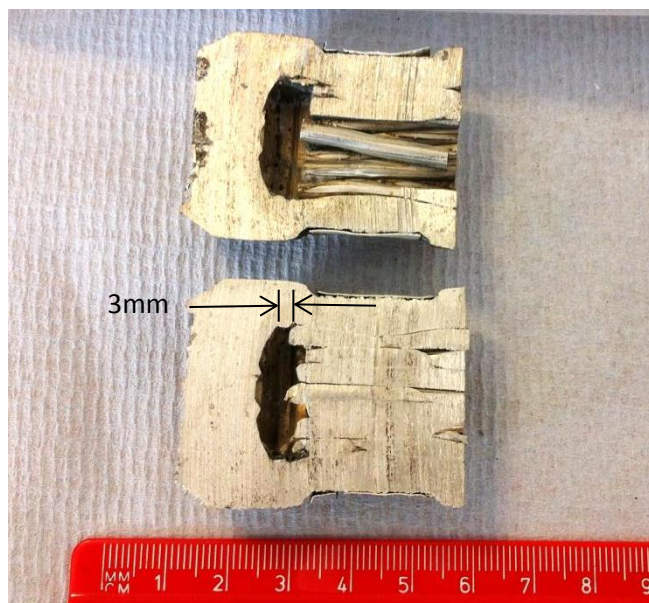


Figure 16: Section through aluminium ferrule, green phase connector

3. Unfailed 11kV Remuera K10 PILC/XLPE transition joint 3-B-0, PN53

3.1 Joint strip down

The joint was of the same design as the failed transition joint on 3-B-0. There was no evidence of an electrical breakdown having occurred in this un-failed joint.

The central red/black insulating sleeves were cut open and removed. The central insulation sleeves did not have an inner semi-conducting layer. The insulation had partly discoloured from the original salmon pink colour to a grey brown colour, Figure 17 and Figure 18.



Figure 17: Central insulating sleeve from un-failed joint



Figure 18: End of insulation sleeve shown in Figure 15

Yellow mastic had been applied over the compression connector and in the voids between the connectors and the core insulation. The yellow mastic was brown and hardened on the PILC side of the joint but maintained more of the original colour and consistency on the XLPE side.

On the PILC cable there was a black heat shrink glove over the cable crutch with yellow mastic in the cable crutch extending over the end of the translucent heat shrink sealing tube and 8mm onto the semi-conducting heat shrink tube. The lead sheath was terminated 30mm away from the end of translucent, oil resisting, heat shrink tubing on each core.

The core numbering papers were still present beneath the translucent heat shrink tubes applied over each core indicating that the jointer had left the full thickness of insulation in place on each core.

The papers were very dry with little evidence of impregnating compound. There were localised blackened areas on the outer core papers, particularly on core 2, but not on the overlying belt papers. From the position of the longitudinal mark, made on site to indicate the top of the cable, the blackened area on core 2 was on the underside of the cable.

Figure 19 shows the blackened area on the outer core identification papers on core 2 extending from the lead sheath cut back position back under the lead sheath for a distance of at least 100mm beneath the belt papers which were not blackened.



Figure 19: Dark surface on core 2 beneath belt papers and lead sheath

A section of discoloured core identification paper from core 2 is shown in Figure 20. As well as being discoloured, the core 2 identification papers tended to crack along the butt gaps.

From the visual examination, three distinct zones were identified on the core 2 identification tapes: the light brown relatively unaffected areas, the areas where the paper was blackened and the areas where there were deposits of what appeared to be blackened impregnating compound on top of the paper. These three zones can be seen in Figure 20.



Figure 20: Section of discoloured core identification paper from core 2

Figure 21 shows the three PILC cable cores after removing the number tapes. The blackening is still visible on core 2, extending from the lead sheath cut back position under the lead sheath for a distance of approximately 55mm.

The three PILC cores shown in Figure 21 were stripped down to the conductor between the end of the translucent heat shrink sealing tube and the PILC cable end. The papers were dry towards the cable end and burnt and oily nearer to the ferrule. The inner papers had a tendency to split along the butt gaps. The conductor strands were slightly bird-caged on the outside of the bend where the jointer had used a temporary spacer to separate the 3 cores.

On core 1 there was dark staining on the layer below the core identification tapes and in subsequent layers in the butt gaps. The conductor strands were generally dry with no evidence of compound but with small amounts of a relatively thin black liquid between the strands in places. There were dark brown "blotches" on the conductor strands near to the end of the translucent heat shrink sealing tube, Figure 22.

On core 2 the black discolouration on the core identification tape did not extend to the underlying layers. The underlying papers were creased and the inner papers tended to split at the butt gaps.

The core 3 papers had dark brown discolouration in the butt gaps beneath the lead sheath but close to the lead sheath cut back position. The papers were dry and brittle with a strong burnt sugar smell. The core 3 papers got darker towards the conductor. The conductor strands were dry with no compound or bitumen contamination. The conductor strands were discoloured with a range of colours from cherry red, through blue to black at a point close to the end of the lead sheath but under the lead sheath, Figure 23. From past experience this type of discolouration of copper is caused by localised overheating.



Figure 21: Three cores of PILC cable with localised discolouration on core 2

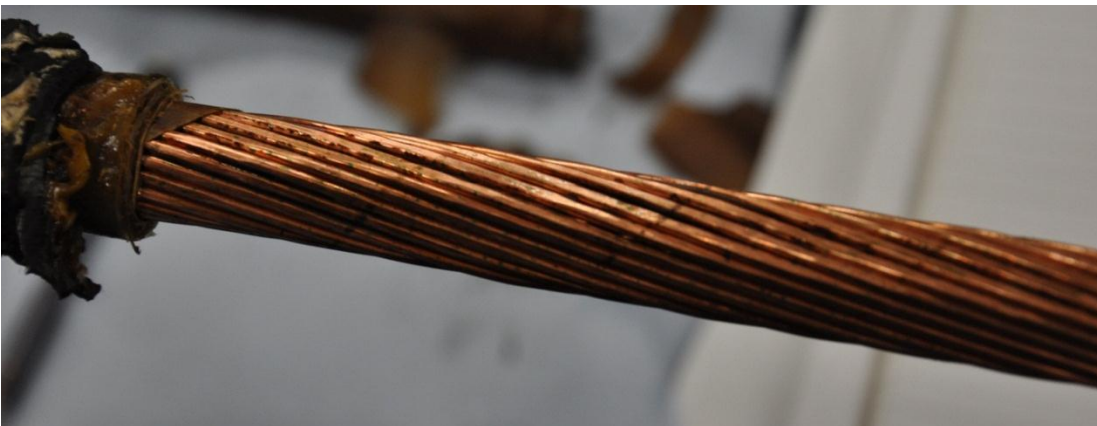


Figure 22: Localised "blotches" on conductor strands on core 1

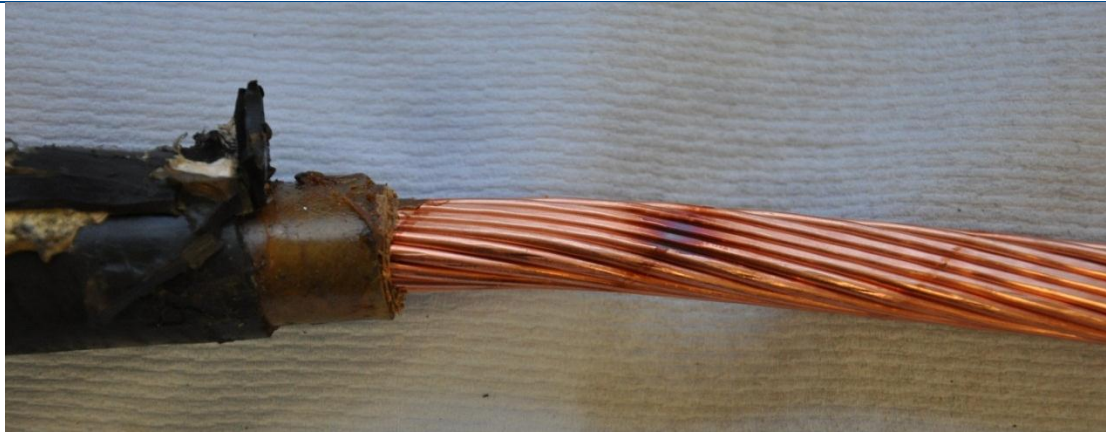


Figure 23: Localised apparent thermal effect on conductor, core 3

The compression ferrules on the bimetallic connectors had been uniformly compressed onto the conductors, Figure 24.

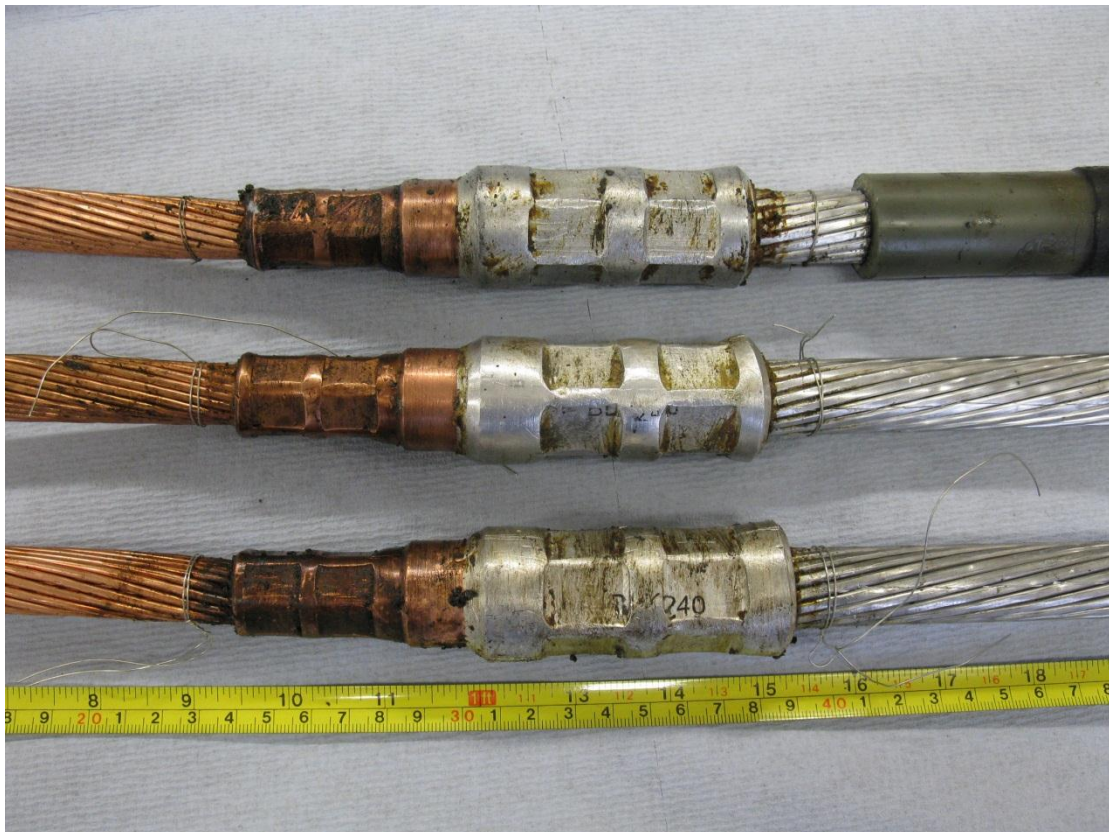


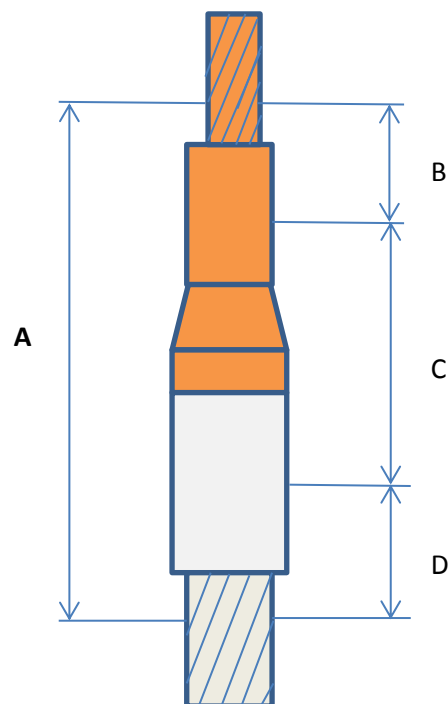
Figure 24: Bimetallic connectors after removing insulation

3.2 Resistance measurements

Resistance measurements were made on the bimetallic connectors using a 4 pole microhmmeter. The results are shown in Table 1. From the author's previous experience designing cable connectors, these are acceptably low values.

Table 1: Conductivity measurements on bimetallic connectors from PN53

Phase	Resistance $\mu\Omega$			
	Conductor to Conductor "A"	Copper Ferrule "B"	Bimetallic Weld "C"	Aluminium Ferrule "D"
Red	16.7	5.8	0.4	10.3
White	21.2	2.8	0.5	18.2
Green	20.3	4.6	0.4	17.4



3.3 Microscopy on PILC cable components

A strand from core 1 with the "blotches" of material on the surface and a discoloured conductor strand from core 3, were examined in the SEM.

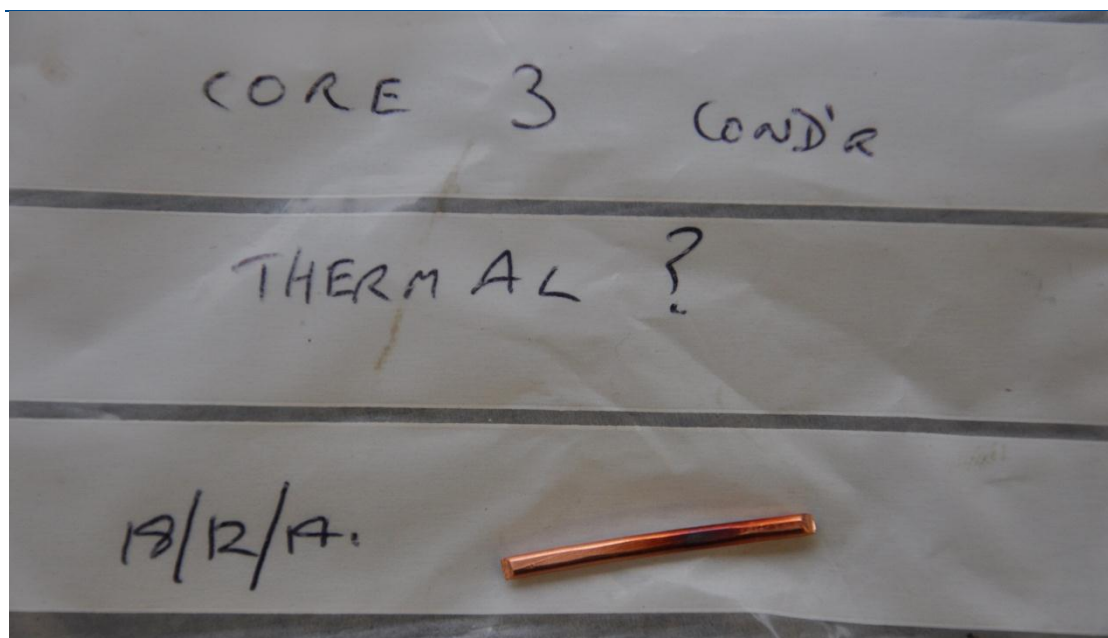


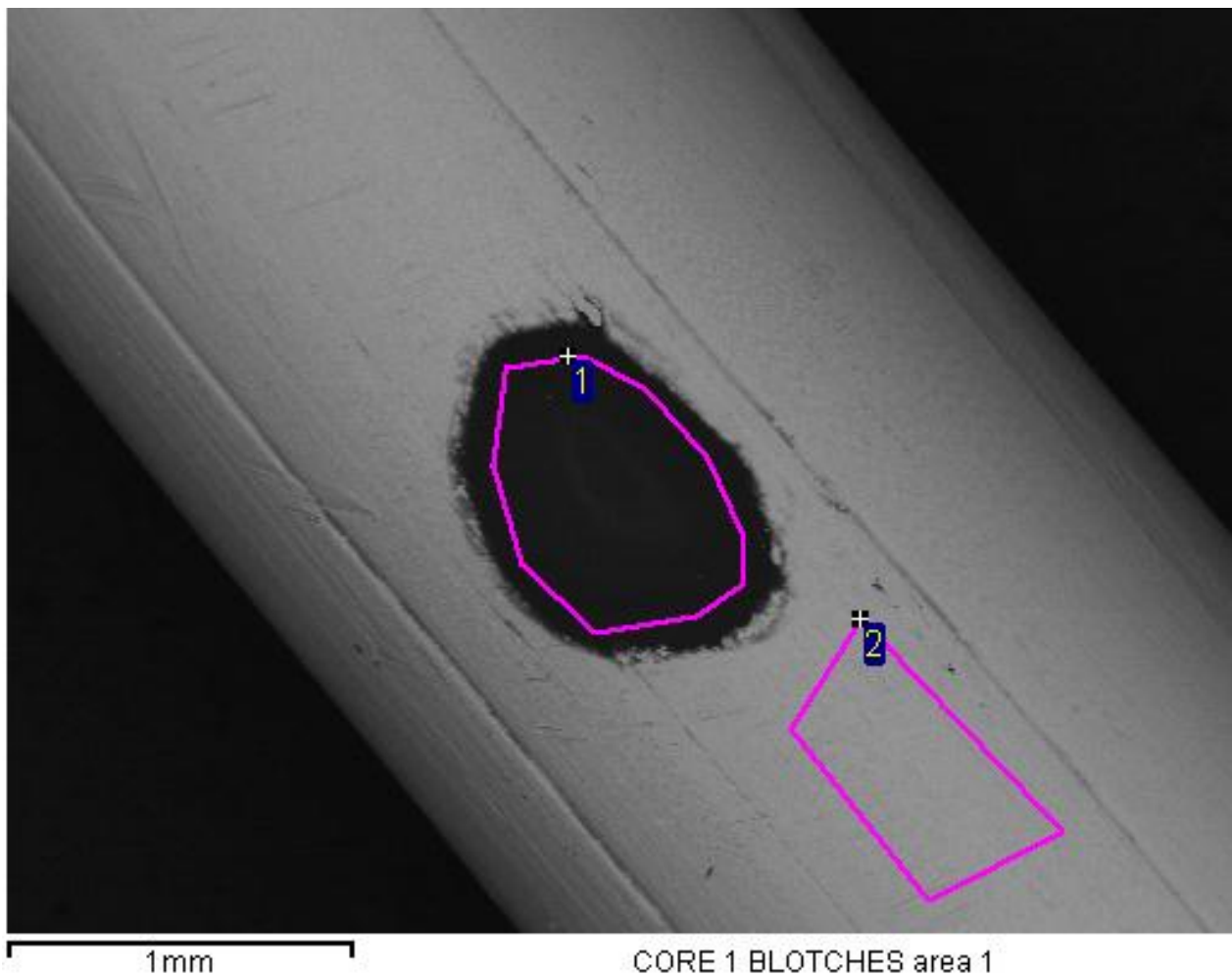
Figure 25: Discoloured conductor strand prior to SEM analysis

The SEM and EDX analysis of the blotches on core 1 showed them to be mainly carbon and oxygen with a small amount of copper. From this result and their visual appearance it is likely that these blotches were areas where the majority of the compound had evaporated due to the heat of the fire and the remaining less volatile components had been baked to the surface of the copper conductor strands.

From the SEM EDX analysis of the discoloured area shown in Figure 25 the discolouration comprised carbon, oxygen and copper. Away from the discoloured region the surface was copper with less than 5% carbon. Considering the conditions this is effectively clean copper.

Where the copper was discoloured there was more than 80% carbon. This indicates that there was a carbon based substance over the top of the copper. The discolouration was not just due to heat causing the copper to oxidise.

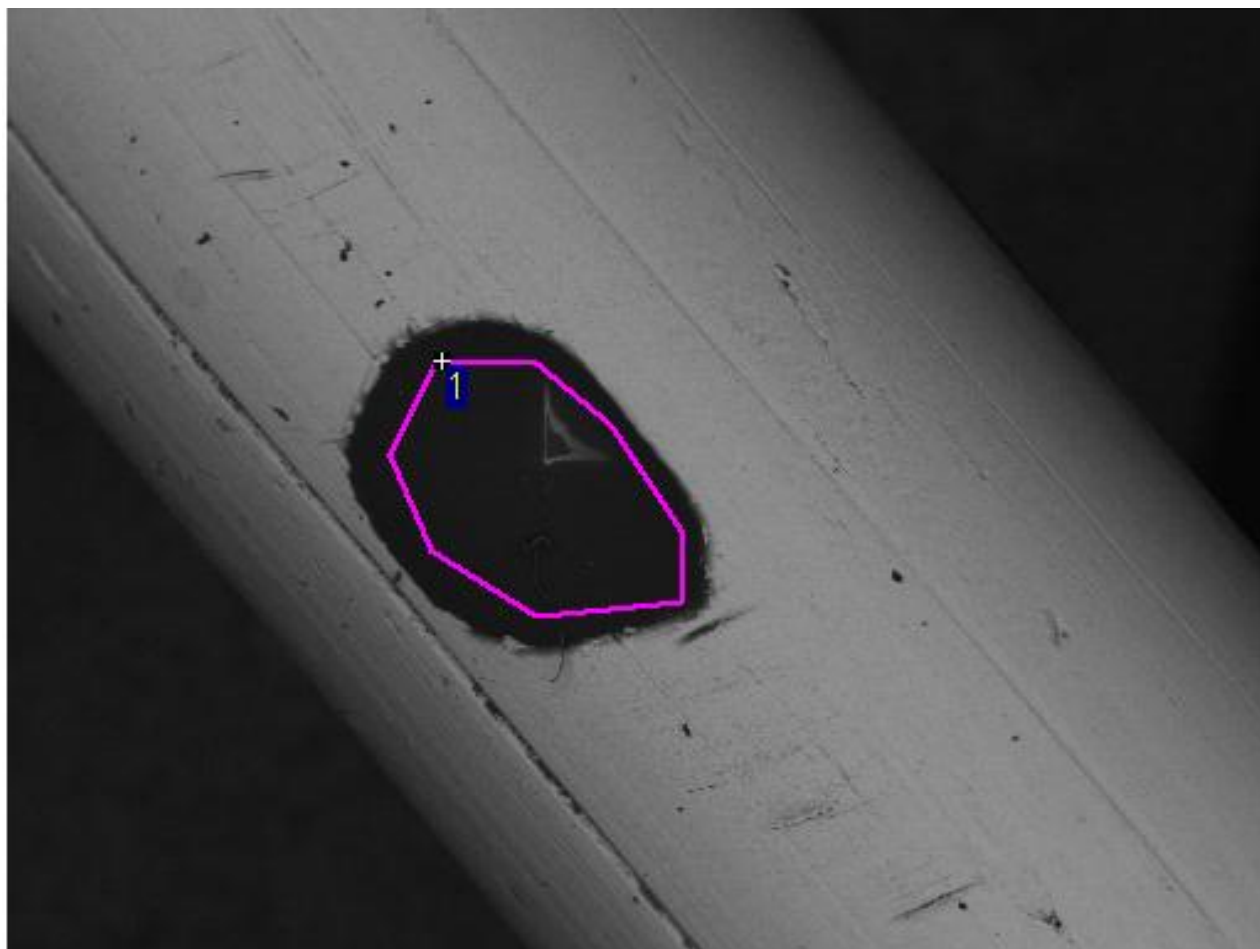
EDP2744001 COPPER STRANDS 12/18/2014 10:45:58 AM



Processing option : All elements analysed (Normalised)

Spectrum	In stats.	C	O	Cu	Total
1	Yes	83.9	11.7	4.5	100.0
2	Yes	9.0	0.5	90.5	100.0
Mean		46.4	6.1	47.5	100.0
Std. deviation		52.9	7.9	60.8	
Max.		83.9	11.7	90.5	
Min.		9.0	0.5	4.5	

EDP2744001 COPPER STRANDS 12/18/2014 10:55:06 AM



1 mm

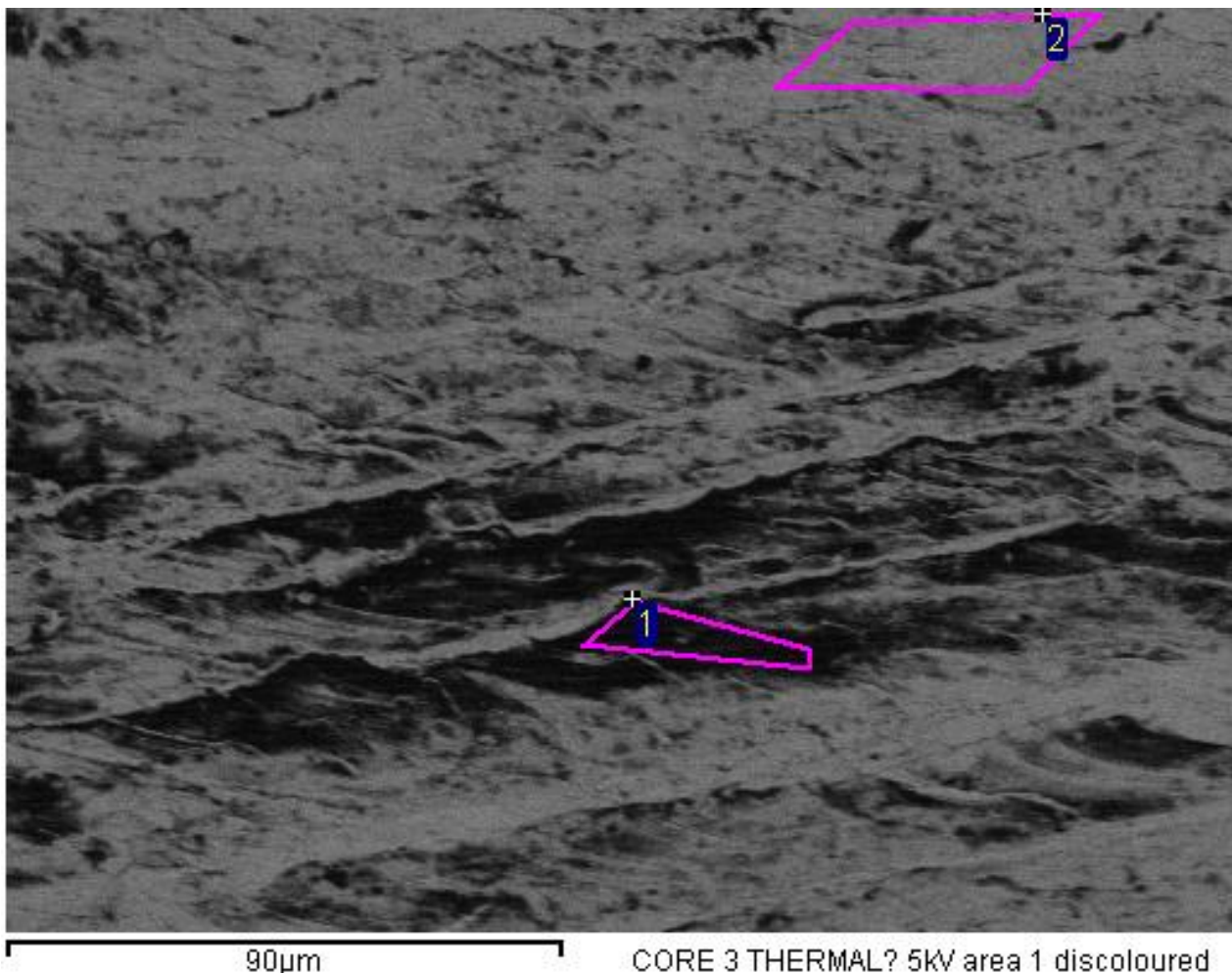
CORE 1 BLOTCHES area 2

Processing option : All elements analysed (Normalised)

Spectrum	In stats.	C	O	Cu	Total
1	Yes	81.5	14.5	4.0	100.0
Mean		81.5	14.5	4.0	100.0
Std. deviation		0.0	0.0	0.0	
Max.		81.5	14.5	4.0	
Min.		81.5	14.5	4.0	

All results in weight%

EDP2744001 COPPER STRANDS



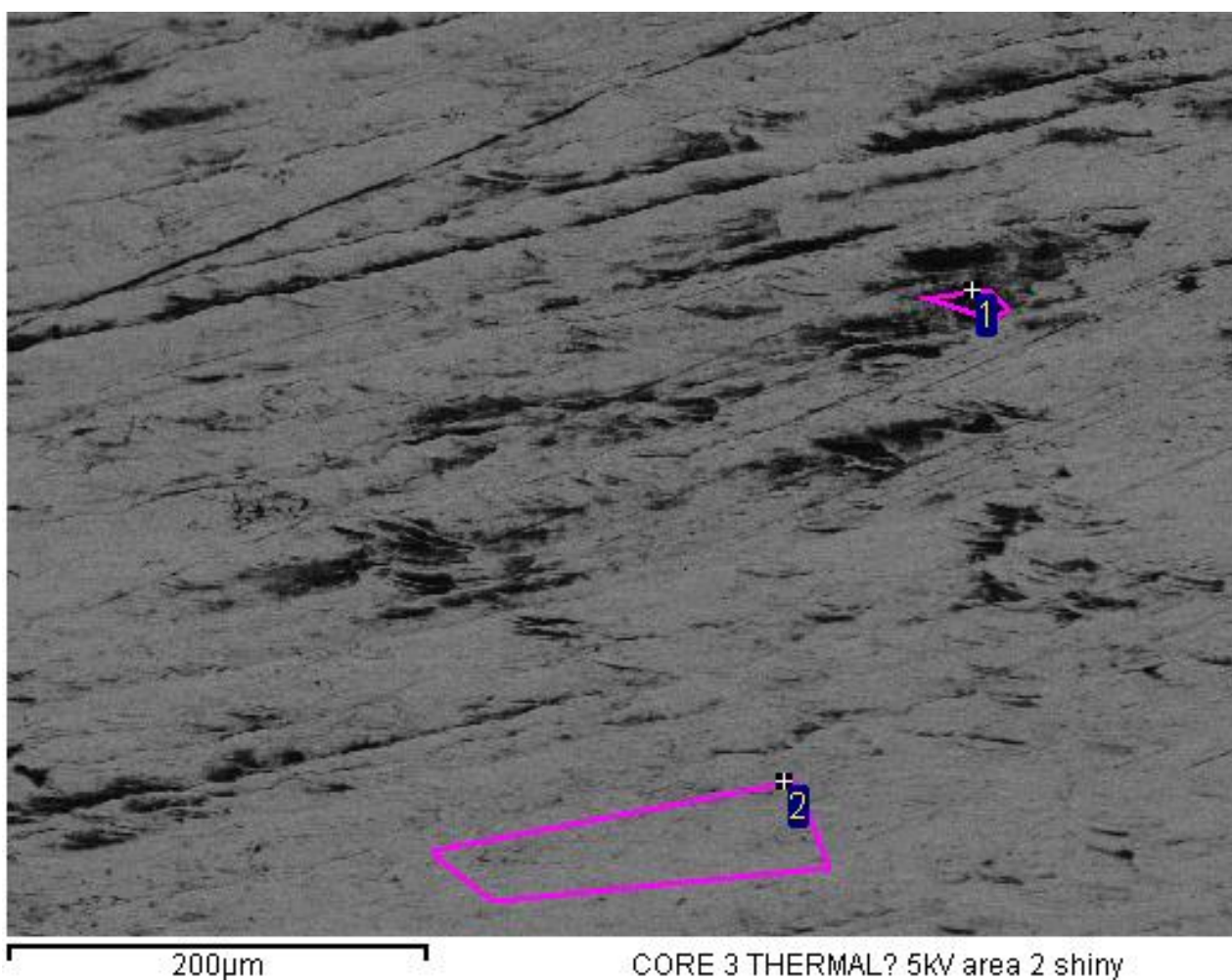
Processing option : All elements analysed (Normalised)

Spectrum	In stats.	C	O	S	Cu	Total
1	Yes	53.7	4.4	3.4	38.5	100.0
2	Yes	4.9	0.5	5.1	89.6	100.0
Mean		29.3	2.5	4.2	64.1	100.0
Std. deviation		34.5	2.8	1.2	36.1	
Max.		53.7	4.4	5.1	89.6	
Min.		4.9	0.5	3.4	38.5	

All results in weight%

EDP2744001 COPPER STRANDS

12/18/2014 11:19:15 AM



Processing option : All elements analysed (Normalised)

Spectrum	In stats.	C	O	S	Cu	Total
1	Yes	54.2	8.1	1.7	36.0	100.0
2	Yes	4.9	0.5	1.3	93.3	100.0
Mean		29.5	4.3	1.5	64.7	100.0
Std. deviation		34.8	5.4	0.3	40.5	
Max.		54.2	8.1	1.7	93.3	
Min.		4.9	0.5	1.3	36.0	

All results in weight%

Close examination and staining of the outer papers on core 2 (taken from the area with the dark feature shown in Figure 19 and 20) indicated waxing, blackening and degradation, Figure 29, of the paper fibres in the butt gaps on core 2 as well as the more widespread blackening away from the butt gaps, Figure 26. The black deposits in the butt gaps could be bitumen from the original cast iron, bitumen filled, cable joint.



Figure 26: Identification paper from core 2, un-failed transition joint



Figure 27: Stained paper with section cut out for SEM analysis

SEM analysis of the blackened outer tapes from core 2 indicated that:

- The un-blackened paper was carbon with some silica particles. The cellulose fibres could be seen as well as a smooth material between the fibres

- The blackened areas all had chlorine, carbon, silicate and oxygen present.
- Where the papers had badly deteriorated, Figure 29, and fractured, the smooth areas that bonded the fibres together, Figure 28, had mainly been lost. These areas also had chlorine, carbon, silicate and oxygen present.

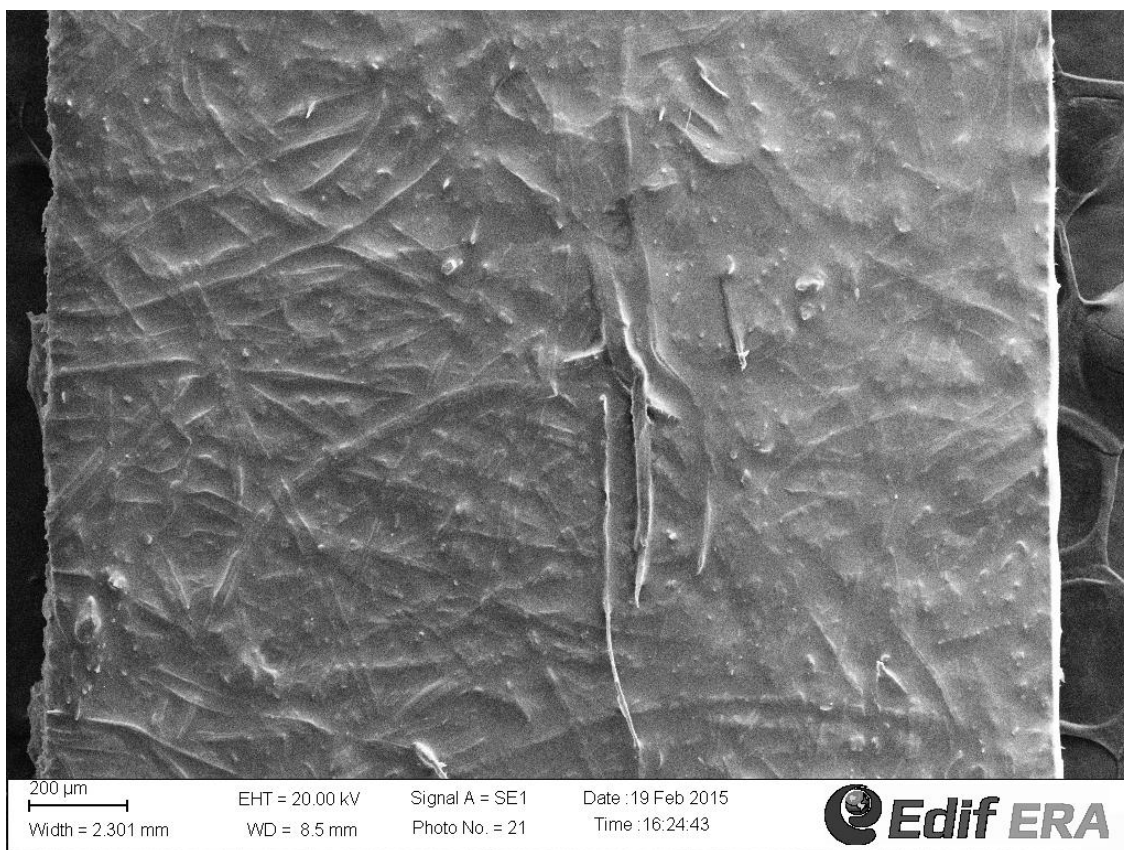


Figure 28: SEM image of paper in relatively good condition

FTIR analysis of the stained area and the yellow mastic confirmed that the yellow mastic was present in the stained feature. The FTIR spectrum for the stained area was not the same as the spectrum for bitumen.

A miscibility test was performed on the yellow mastic material in hydrocarbon insulating oil. This confirmed that the yellow mastic was not readily miscible.

The relative permittivity of new yellow mastic material was tested three times at low voltage and measured to be 12.9, 10.7 and 11.9, average 11.8.

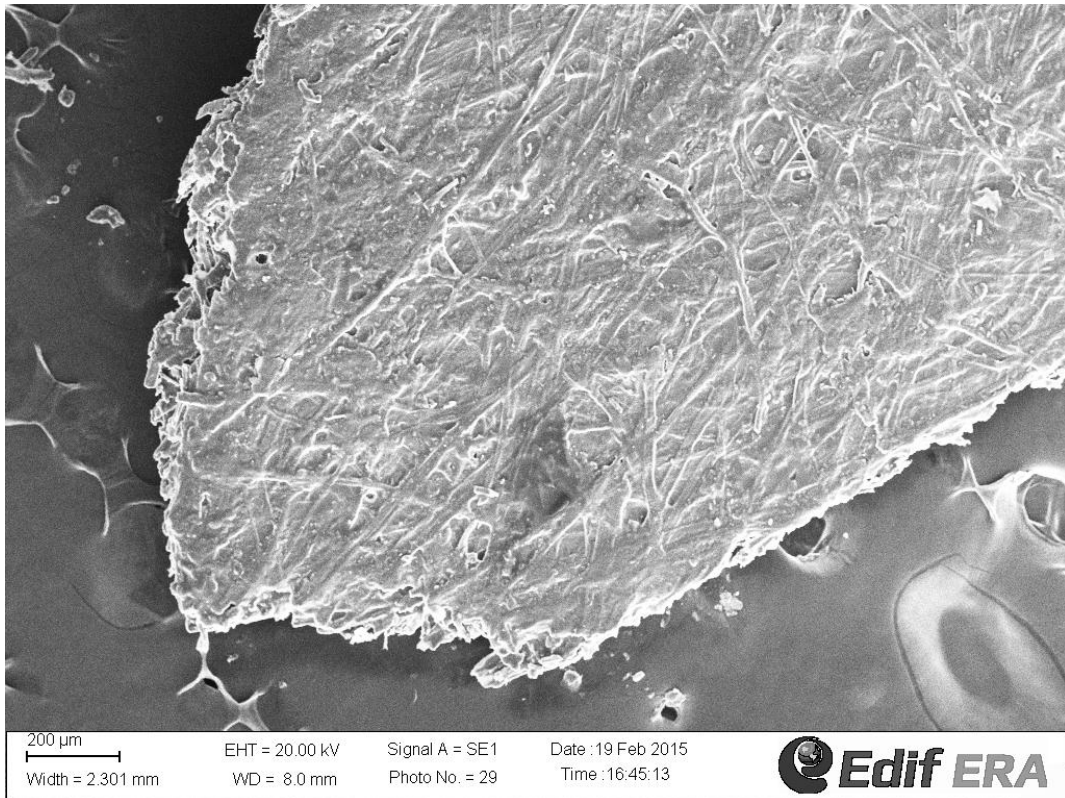


Figure 29: SEM image of fractured edge of degraded paper

3.4 Tensile testing

Tensile tests were performed on the red and green labelled connectors by applying a tensile load to the aluminium and copper stranded conductors, Figure 30.



Figure 30: Tensile test on red phase bimetallic connector from PN53

The tensile test results are shown in Table 2.

Table 2: Tensile tests on bi-metallic connectors from PN53

Connector	Time at 9.7kN (s)	Time at 12kN (s)	Failure load (kN)	Comments
Red	60	60	N/A	No failure occurred
Green	60	N/A	10,918	Aluminium conductor pulled out of connector ferrule

3.5 Examination and testing of bimetallic welds

The red and green labelled connectors were split longitudinally so that the bimetallic welded interface could be examined.

There was no evidence of any separation at the aluminium/copper interface and no evidence of a heat affected zone where the two elements were combined, Figure 31.

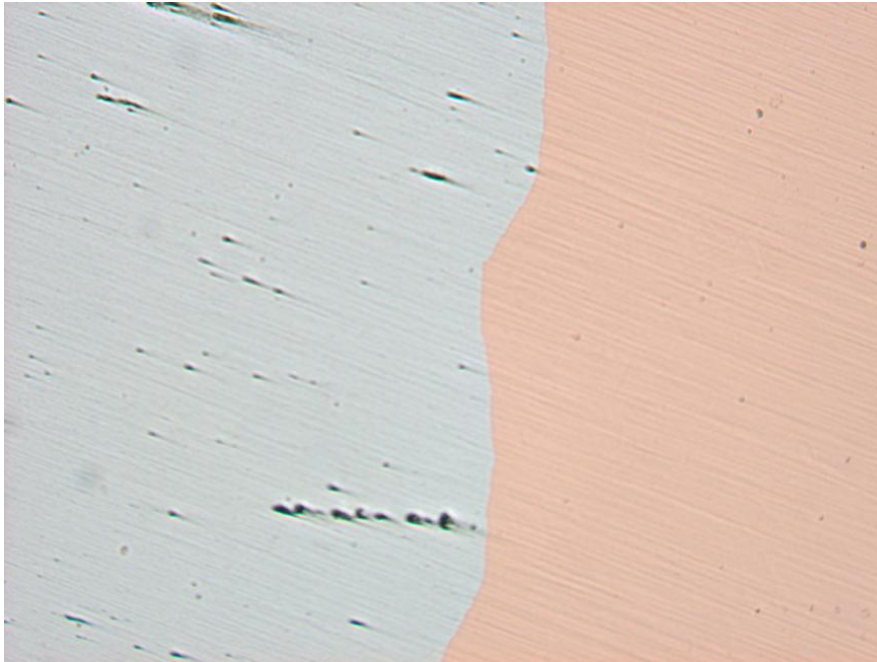
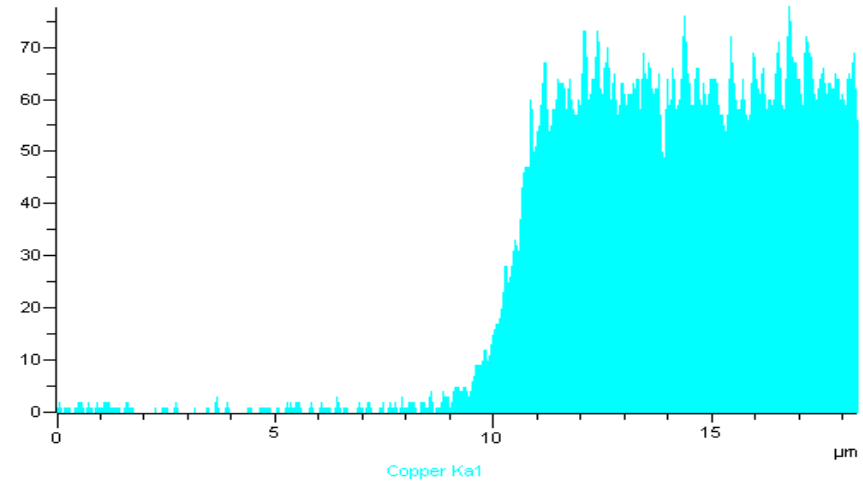
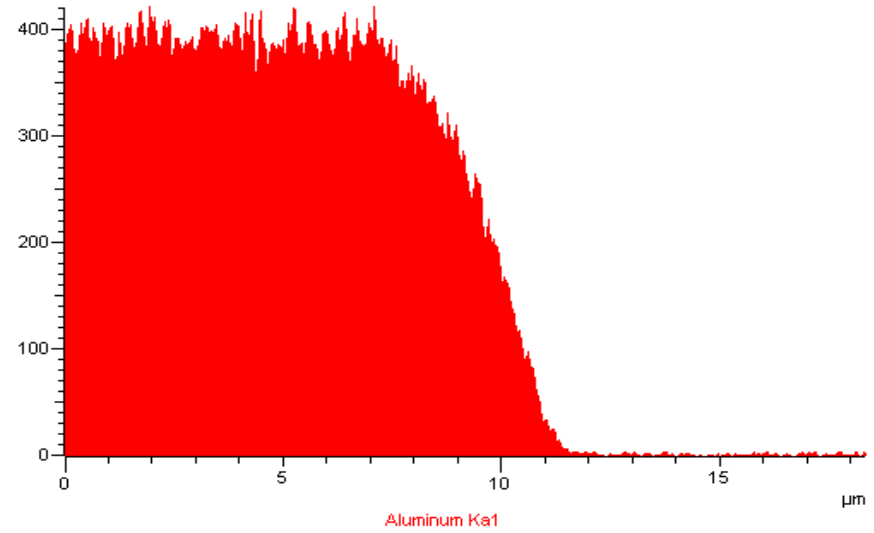
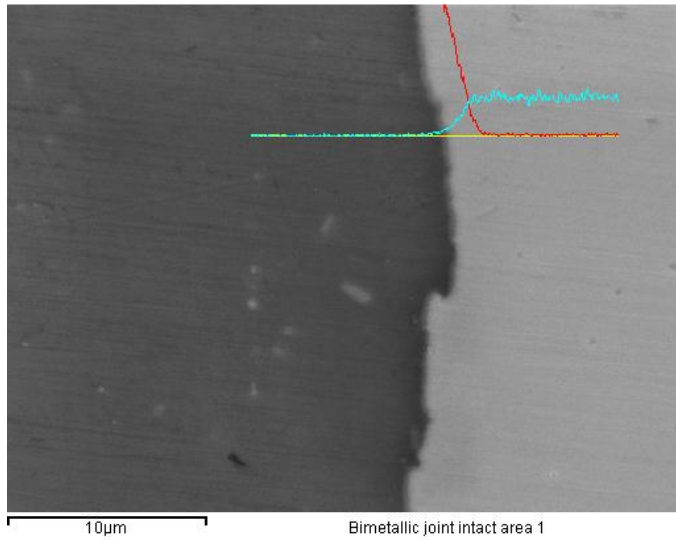
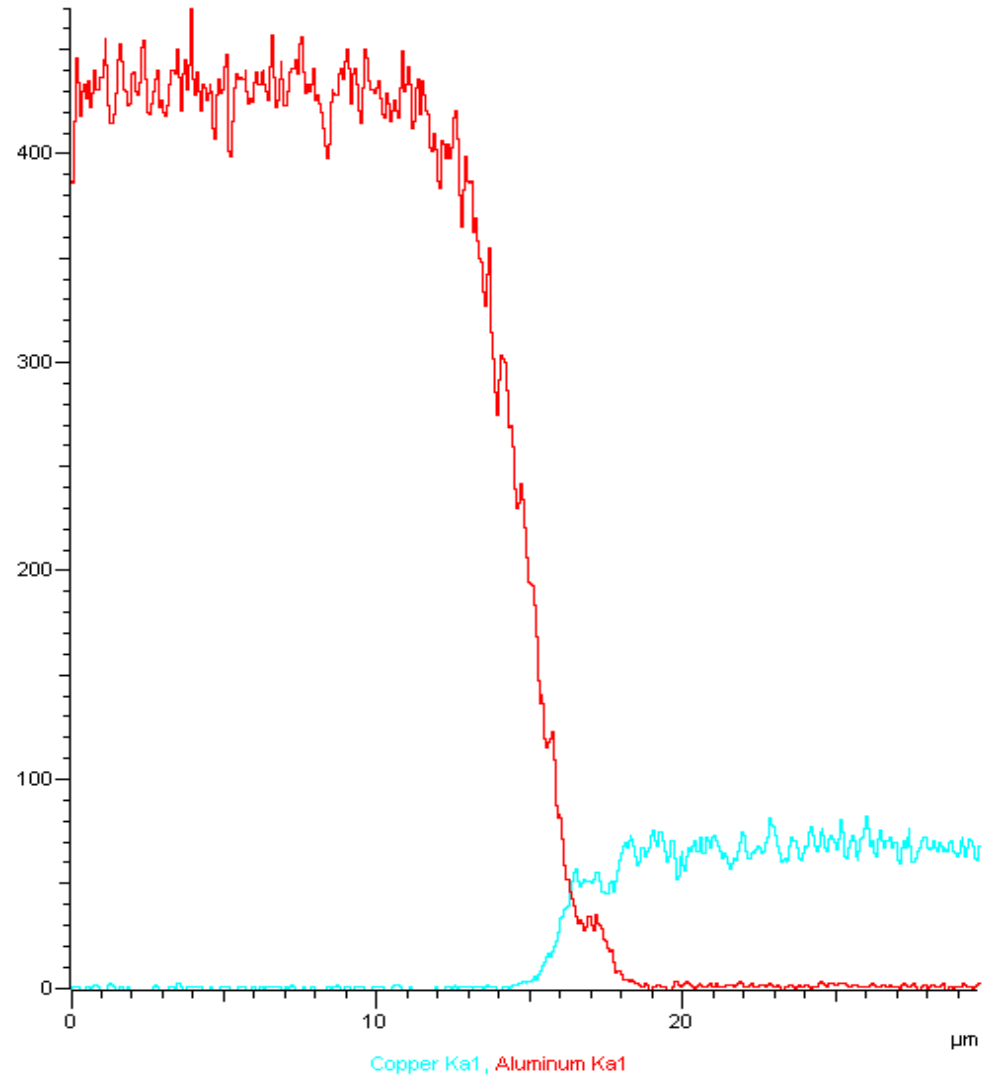
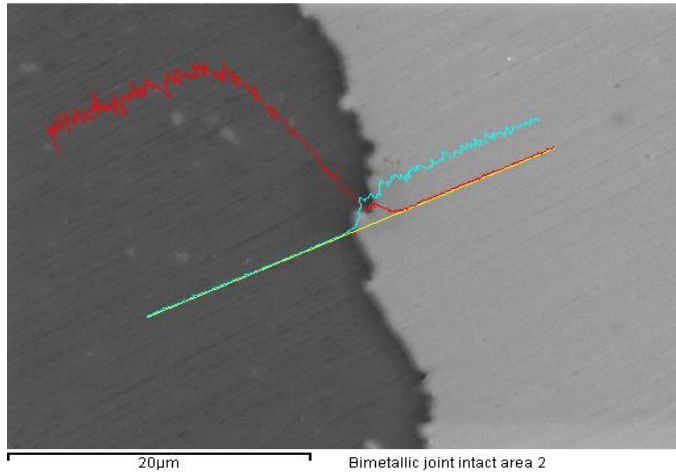


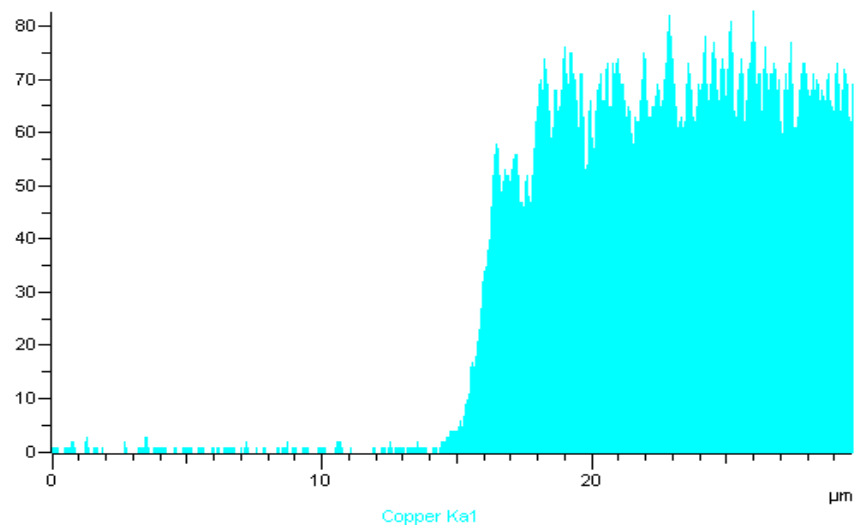
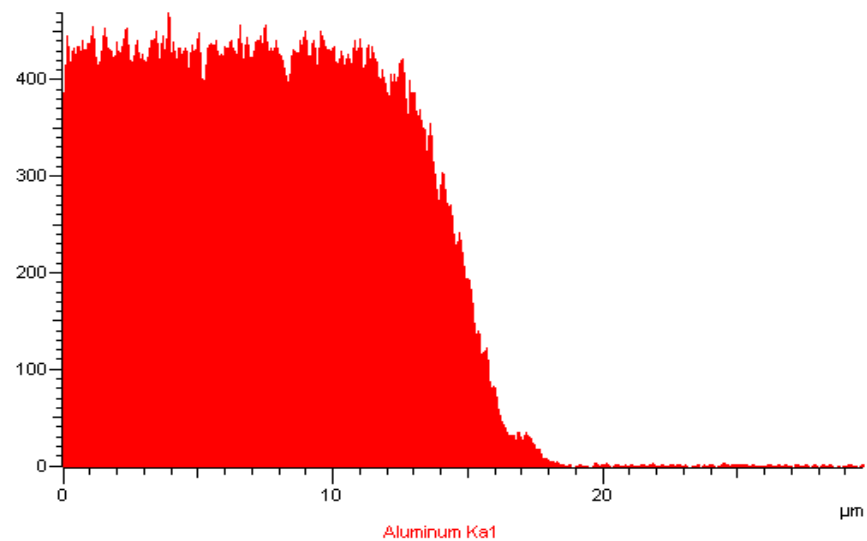
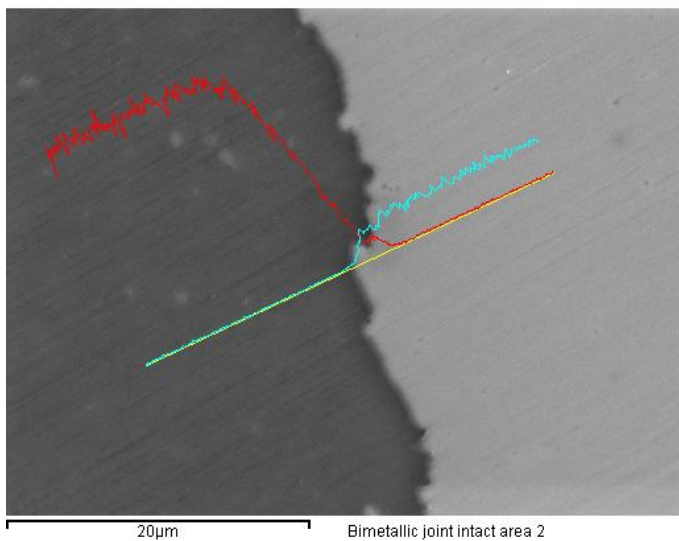
Figure 31: Red connector aluminium/copper interface (scale approx. 1mm from top to bottom)

The apparent voids and scratches in Figure 31 were due to the cutting process used to separate the connector longitudinally. One half of the green connector was polished to obtain a smooth surface and examined in the SEM. From the SEM results:

- The distance between the helical ridges in the copper half of the connector was 0.6mm. The ridges were visible along the welded interface.
- At the interface there was a very thin (2 μ m thick) zone where aluminium occurred in the copper. However this could be a result of the polishing process used by ERA rather than a result of the welding process.
- There was no evidence of copper in the aluminium.
- There were some areas where the copper and aluminium had become locked together mechanically as a result of the way the surfaces had deformed, see following SEM images.







The two halves of the red labelled PN 53 connector were subjected to a transverse load in a tensile testing machine.

The connector was held horizontally with the copper half clamped on the base of the tensile test machine. A vertical load was applied to the aluminium side 75 to 80mm from the copper/aluminium interface, Figure 32 and Figure 33. In both cases the aluminium ferrule bent without the aluminium/copper interface separating.

The connector halves were then turned over and the load applied at the same distance from the interface from the other side causing the weld to separate. In both cases there was aluminium visible on the copper side of the interface, see Figure 34.



Figure 32: Initial arrangement for testing bi-metallic weld on PN 53 connector



Figure 33: Initial loading arrangement



Figure 34: Weld interface surfaces showing aluminium adhering to copper surface

The results of the axial load tests on the weld are shown in Table 3.

Table 3: Transverse tests on bi-metallic weld on PN 53 connector

Sample Ref.	Ferrule loading arrangement	Applied load, kN	Approximate distance from weld, mm	Observations
Red 1		1.11	77.5	Aluminium ferrule bent. Weld did not fail
		2.04	40	Weld parted
Red 2		2.25	40	Aluminium ferrule bent. Weld did not fail
		1.53	40	Weld parted but two halves remained connected, see fig. 30

One half of the green phase connector from PN53 was held horizontally in a vice in an oven, Figure 35, and the oven heated to 600°C.

After 15 minutes at 600°C the oven door was opened and it was observed that the aluminium half of the connector had separated from the copper half and fallen onto the floor of the oven,

**Figure 35: Half of connector from PN53 mounted in oven**



Figure 36: Half of connector from PN53 after 15 minutes at 600°C

The exposed bi-metallic weld surfaces were examined. There was no visible copper on the surface of the aluminium but there was a thin layer of aluminium on the weld surface of the copper side of the connector.

3.6 Further analysis of crimps on PN33 and PN53 connectors

Measurements of the conductor diameter and the connector diameter were taken at both a crimped depression and an un-crimped full diameter section of each of the PN 33 and PN53 connectors, Figure 43. The measurements at depressions were taken in line with the flats of the compression. These measurements are given in Table 4 and Table 5.

Table 4: Degree of achieved compression measurement at depression

Sample	Cu inner, mm	Cu outer, mm	Ratio	Al inner, mm	Al outer, mm	Ratio
PN53 Red 1	13.86	-	-	17.60	29.85	0.59
PN53 Red 2	13.58	-	-	17.56	29.30	0.60
PN53 Green 1	14.07	21.03	0.67	18.35	29.33	0.63
PN53 Green 2	-	-	-	18.66	29.60	0.63

Sample	Cu inner, mm	Cu outer, mm	Ratio	Al inner, mm	Al outer, mm	Ratio
PN53 White	14.81	21.49	0.69	19.18	29.25	0.66
PN33 Red	15.33	21.50	0.71	18.99	29.53	0.64
PN33 Green	14.85	21.33	0.70	18.93	29.85	0.63
PN33 White	15.20	21.07	0.72	18.94	29.57	0.64

Figures in red signify distorted by previous testing or not squarely cut

Table 5: Degree of achieved compression measurement at non-depression

Sample	Cu inner, mm	Cu outer, mm	Ratio	Al inner, mm	Al outer, mm	Ratio
PN53 Red 1	15.19	-	-	20.61	33.89	0.61
PN53 Red 2	15.42	-	-	21.03	34.10	0.62
PN53 Green 1	15.51	22.61	0.69	20.59	33.13	0.62
PN53 Green 2	-	-	-	21.39	33.63	0.64
PN53 White	15.02	22.72	0.66	21.16	34.11	0.62
PN33 Red	15.61	23.89	0.65	20.93	33.46	0.63
PN33 Green	15.95	22.85	0.70	21.22	33.34	0.64
PN33 White	15.88	24.17	0.66	21.56	34.09	0.63

Figures in red signify distorted by previous testing or not squarely cut

The degree of compaction of the conductor strands in the ferrules of each of the connectors, apart from those that had been tensile tested, was also assessed visually. Both the aluminium and copper sides of the PN 33 red and white connectors appeared well compacted, with only small gaps visible between strands, Figure 37, Figure 38, Figure 39 and Figure 40.



Figure 37: PN 33 (failed joint) Good compaction on Red Al, crimped section



Figure 38: PN 33 (failed joint) Good compaction on Red Cu, crimped section



Figure 39: PN 33 (failed joint) Good compaction on white Al, crimped section



Figure 40: PN 33 (failed joint) Good compaction on white Cu, crimped section

Larger gaps were observed between the strands of the PN33 green connector copper section and the PN53 white connector copper section, Figure 41 and Figure 42.



Figure 41: PN 53 white, copper, crimped section



Figure 42: PN 33 green, copper, crimped section

The connectors were sliced longitudinally using a high speed rotary cutter prior to the transverse mechanical tests. This exposed the interface surfaces between the compression ferrule and the

conductor strands from which it was possible to determine the extent to which the conductor strands had been inserted into the compression ferrules, Figure 43, Figure 44 and Figure 45.

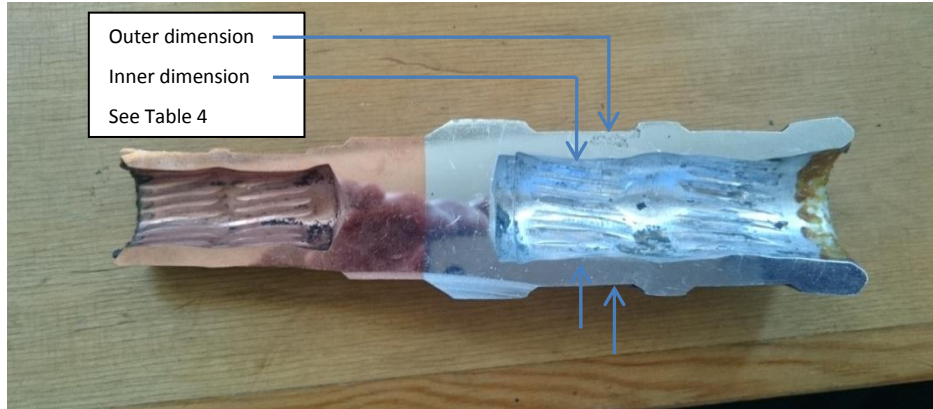


Figure 43: PN53 Green connector with good conductor insertion and compaction



Figure 44: PN53 Red connector with good conductor insertion and compaction



Figure 45: PN53 White connector with conductor strands fully inserted into ferrules

The longitudinal impressions on the cut copper surface in Figure 44 were due to the way the sample had been clamped after it was cut open.

There was black contamination on the inside of the red and white compression ferrules. The white and red connectors had both been partially exposed by thermal degradation of the heat shrink sleeves. The green connector was still covered by a heat shrink sleeve and so may have been less affected by the fire.

4. Examination of nuts and studs from cable trench

Edif ERA received a number of bolt and nut samples labelled PN64 to PN68, Figure 46 to Figure 50. They were examined and tested at ERA. The images shown in Figure 46 to Figure 48 were taken during the examination in New Zealand.



Figure 46: PN64 top bolt 69.5m (Failed Support Position)



Figure 47: PN65 bottom bolt 69.5m (Failed Support Position)



Figure 48: PN66 two nuts 69.5m (Failed Support Position)



Figure 49: PN67 bottom stud and nut 69m



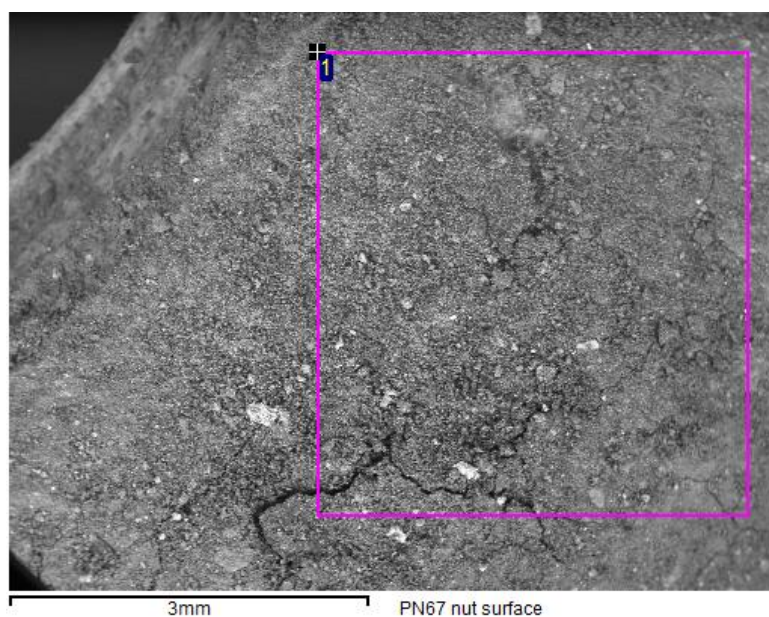
Figure 50: PN68 top stud and nut 69m

A fragment of nut was confirmed to be present on the top stud as shown in Figure 54. A nodule was also present on the top stud indicative of arcing and local melting Figure 59.

From their measured dimensions the nuts and studs were all 5/8" Whitworth.

The stud and nut samples had a mixed zinc and iron oxide layer also containing mineral debris and chlorine. This layer would be consistent with the parts having been exposed to a fire and any subsequent water used to suppress the fire. The high chlorine content is most likely associated with burning of PVC or other chlorinated polymer. Copper was also detected on the surface. Copper would not be expected to be present as an alloying addition in the steel of the nut or bolt at the concentration seen. It is therefore likely that the copper contamination originated from arcing by-products from the cables.

Both the nuts and the studs were galvanised.



All elements analysed (Normalised) – all results in weight%

Area	O	Al	Si	S	Cl	Ca	Ti	Fe	Cu	Zn	Total
1	35.2	6.6	7.3	2.9	5.2	2.7	0.5	9.8	2.1	27.7	100.0

Figure 51: PN67 Nut surface



All elements analysed (Normalised) – all results in weight%

Area	C	O	Al	Si	Cl	Ca	Fe	Zn	Total	Comment
1		24.9	0.6	1.4	7.7	1.3	2.2	61.9	100.0	Thread valley
2	20.5	4.1					50.2	25.1	100.0	Thread tip with metal surface exposed

Figure 52: PN67 Thread surface

There was evidence of the galvanising layer splitting at thread tips and blistering of the galvanised layer on the nuts (see images above). Both indicate that the parts have been exposed to high temperature that has led to softening and bubbling of the zinc layer during formation of the high temperature oxide. The literature suggests that this damage will be encountered when the localised temperature exceeds 250-350 °C, references 2, 3 and 4.

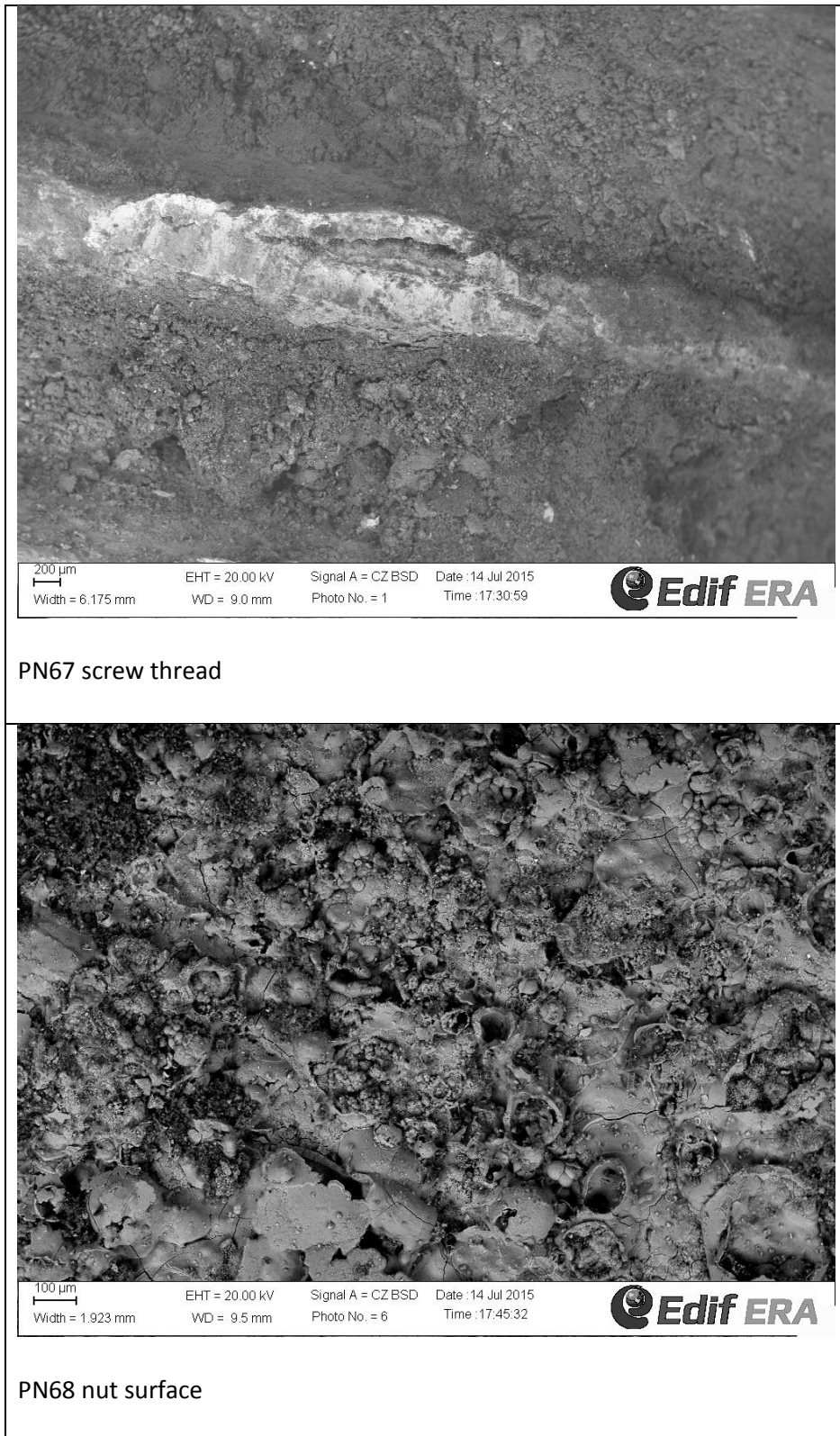
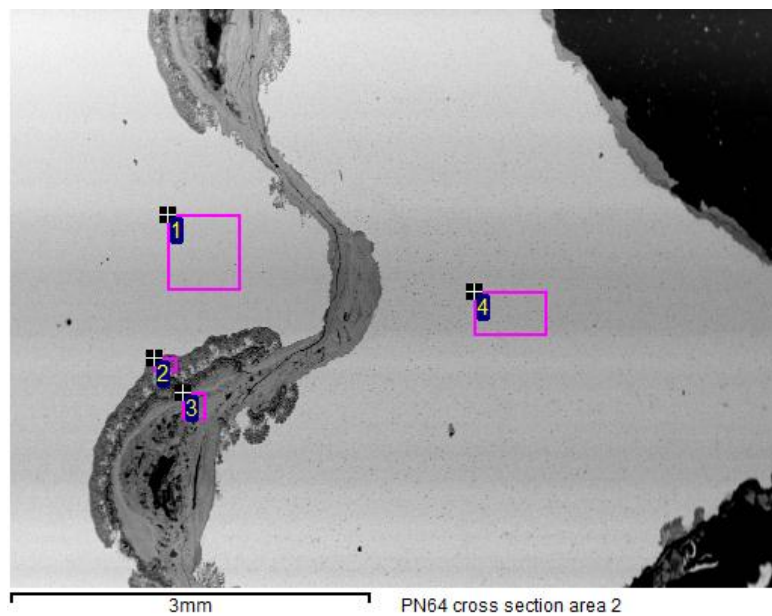
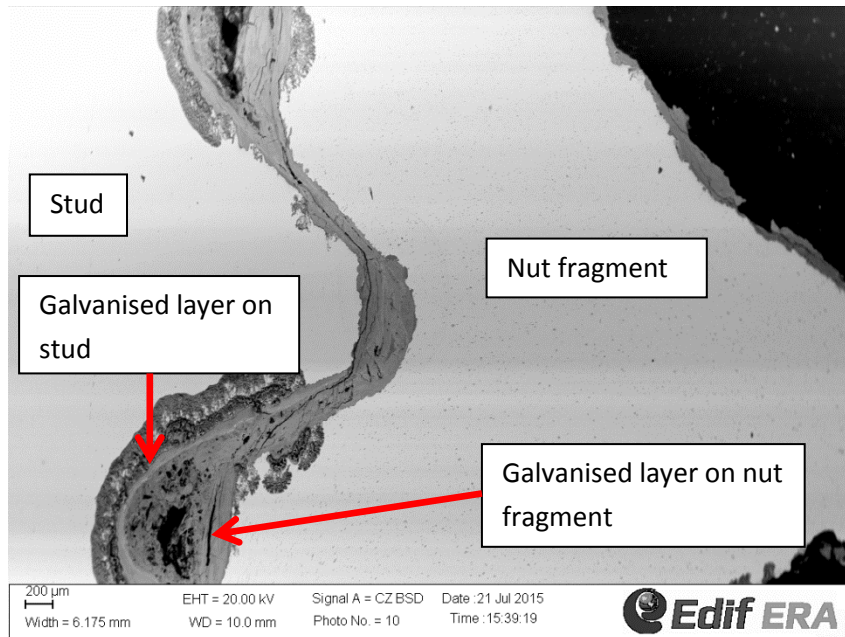


Figure 53: Damage to galvanised layer due to temperatures above 250-350°C

A polished cross-section through PN64 showed evidence of a nut fragment on the stud thread, .

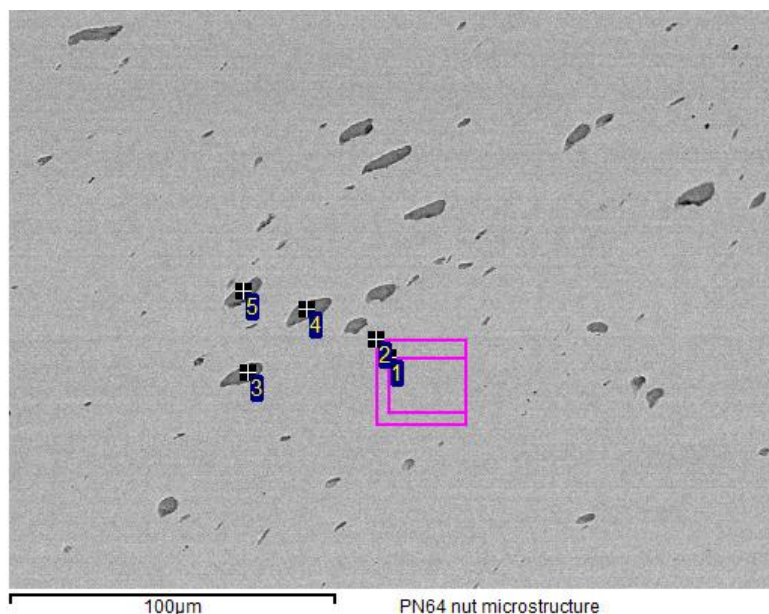


All elements analysed (Normalised) – all results in weight%

Area	O	Si	S	Cl	Ca	Mn	Fe	Zn	Total	Comment
1			0.2			0.4	99.4		100.0	Bolt bulk composition
2	22.6			1.4			76.0		100.0	Oxide layer on bolt
3	27.3	1.1			2.4	0.6	51.8	16.7	100.0	Galvanising layer
4			0.7			1.7	97.6		100.0	Nut composition

Figure 54: PN64 SEM images and chemical analysis

Standard carbon manganese steel had been used on the studs. Free cutting steel (with sulphur addition) had been used for the nut (see Figure 55 below showing backscattered electron image of microstructure, including spherical manganese sulphide particles associated with additions of sulphur to the alloy to improve its machinability).



All elements analysed (Normalised) – all results in weight%

Area	S	Mn	Fe	Total	Comment
1			100.0	100.0	Steel matrix
2		0.9	99.1	100.0	Steel matrix
3	37.3	59.6	3.1	100.0	MnS particle
4	38.3	59.7	2.0	100.0	MnS particle
5	37.7	59.2	3.1	100.0	MnS particle

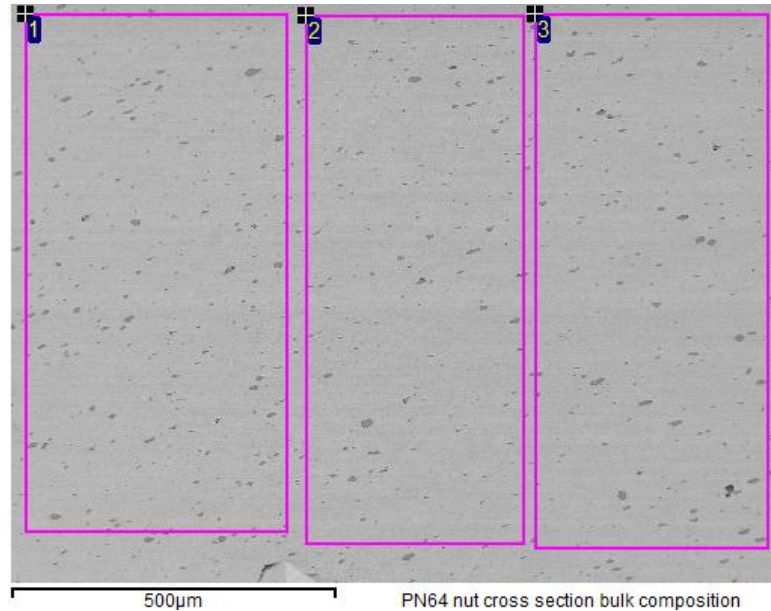
Figure 55: PN64 nut microstructure

The hardness of the stud was 131 ± 7 HV. The hardness of the nut was 208 ± 14 HV.

The specification to which the stud and nut were supplied is unknown. However, ISO 898-1 is the general international standard for the mechanical properties of fasteners made of carbon steel and alloy steel.

If the bolts were supplied to this specification, the measured hardness would indicate that the studs may be either grade 4.6 or 4.8. Grade 4.6 has a minimum hardness of 120HV (Yield strength 240MPa) and grade 4.8 has a minimum hardness of 130HV (Yield strength 320MPa). Free cutting steels are permitted for these specific grades provided the sulphur content does not exceed

0.34wt%. The measured composition of the nut is shown below, Figure 56. The sulphur content of this nut exceeded the permitted level for grades within ISO 898-1.



All elements analysed (Normalised) – all results in weight%

Area	S	Mn	Fe	Total
1	0.60	1.85	97.55	100.00
2	0.48	1.49	98.03	100.00
3	0.62	1.83	97.55	100.00
Mean	0.57	1.72	97.71	100.00
Std. deviation	0.08	0.21	0.28	

Figure 56: PN64 nut SEM image and bulk composition

The etched microstructures of the studs and bolts are shown below, Figure 57. These consisted of pearlite islands (dark phase) within a ferrite matrix (light phase).

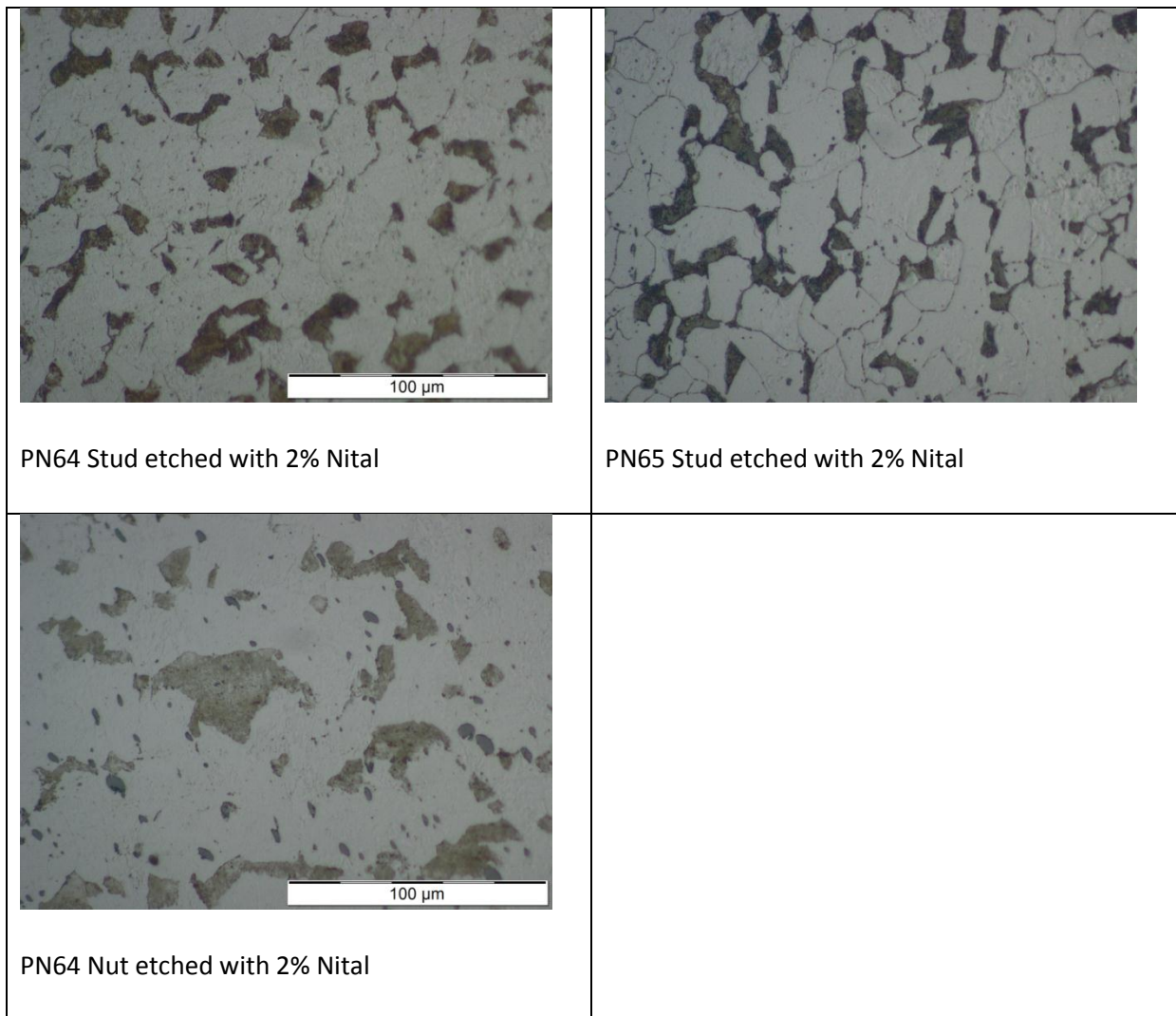


Figure 57: PN64 and PN65 microstructure

Detail of the lamellar spacing within the pearlite indicated that the material had not been exposed to high temperature $>500^{\circ}\text{C}$ for any prolonged time period as there was no spheroidization of the pearlite.

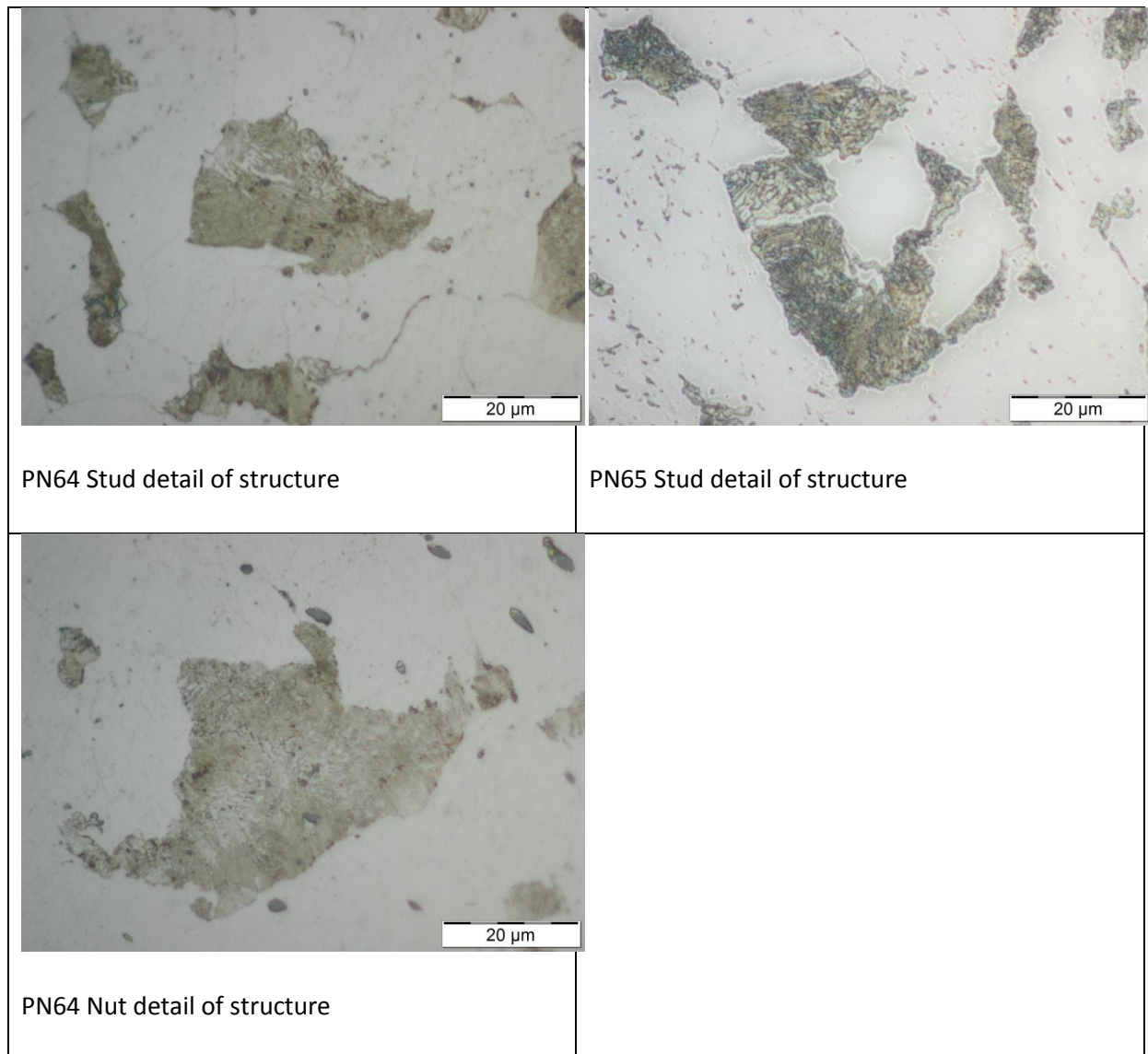


Figure 58: Higher magnification views of PN64 and PN65 pearlite microstructure

Examination of the stud surface therefore suggests that the extensive damage was associated with arcing to the stud and bolt, producing a temperature sufficiently high to melt the surface but of an insufficient duration to alter the internal structure of the steel. Had the damage been associated with an intense fire for a prolonged period, spheroidization of the pearlite in the metal would be observed together with melting/loss of the galvanised layer between the stud and nut. Neither of these features was present.



Figure 59: Surface nodule on Stud PN64 indicative of arcing and localised melting

The PN66 nut threads showed no significant damage, other than the surface corrosion seen on all studs and bolts. It is unclear if the nuts had been positioned on studs at some time. However, the intact nature of the threads and the zinc galvanising layer indicate that the nuts did not detach from the studs at raised temperature during any “fire event.” More significant damage to the thread and galvanising layer would be expected and probably some evidence of stud thread residue would be visible on the nut.

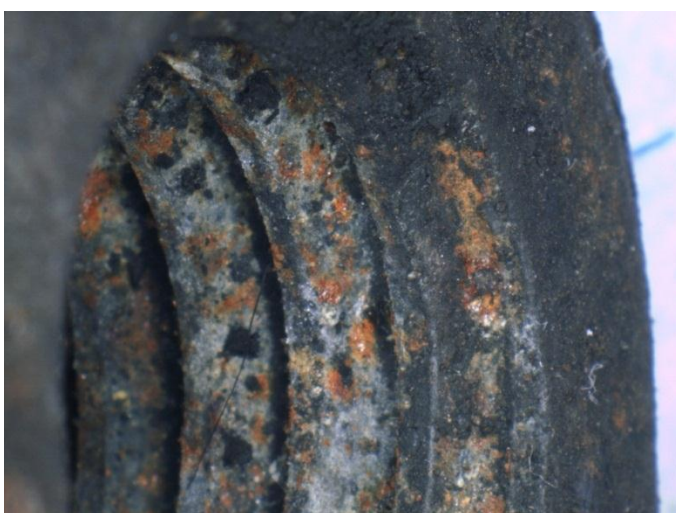
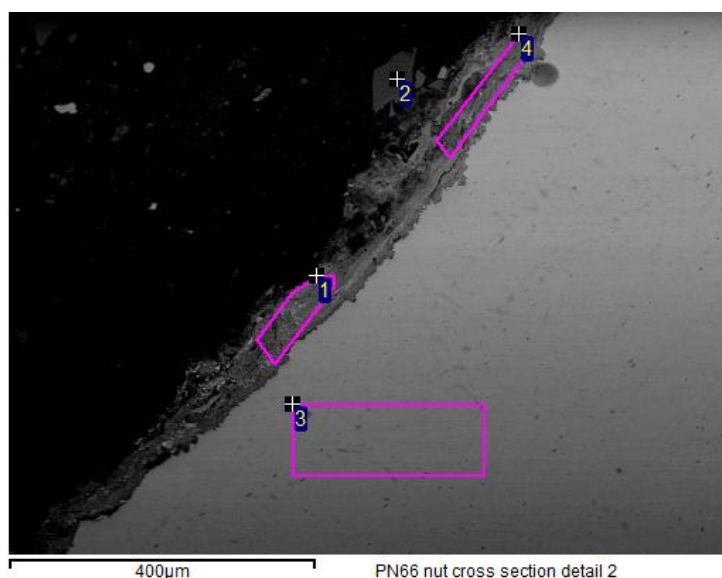


Figure 60: Surface corrosion on PN66 nut screw-threads

Chlorine was detected at high concentration on both the outer galvanising surfaces and the thread surfaces. It is expected that this chlorine is a contamination from the cable fire event (caused by the burning of a chlorinated polymer cable sleeve). The presence of chlorine on all nut surfaces would therefore suggest that the nut was not attached to a stud at the time of the fire.

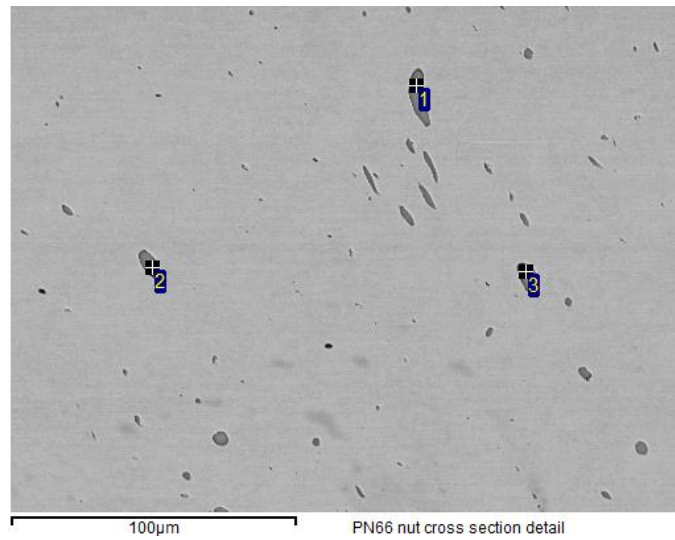


Area	C	O	Na	Al	Si	Cl	Ca	Mn	Fe	Zn	Total
1		18.6				10.3			20.8	50.3	100.0
2	3.8	45.0	6.3	11.1	31.4		2.5				100.0
3	3.6							1.5	95.0		100.0
4		22.0		1.0	2.5	11.2			34.9	28.4	100.0

Figure 61: PN66 nut cross section and SEM analysis

The measured hardness of one of the PN66 nuts was 143 ± 10 HV.

Free cutting steel (sulphur addition) had also been used for these nuts (see image below, Figure 62, again showing backscattered electron image of microstructure, including spherical manganese sulphide particles associated with additions of sulphur to the alloy to improve its machinability).

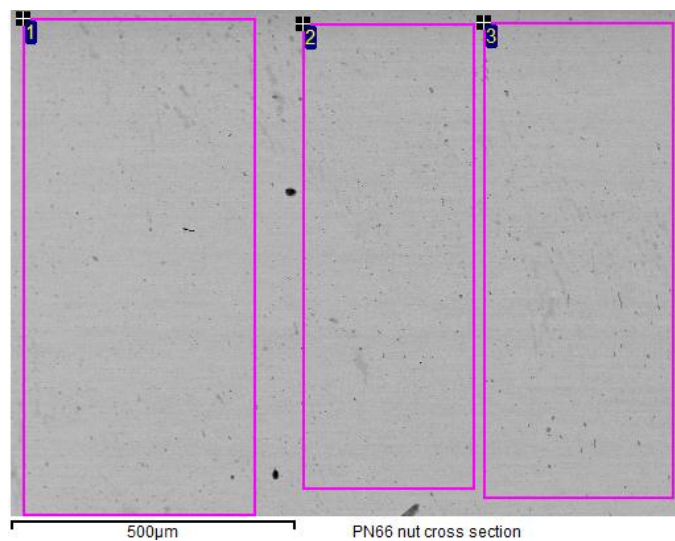


All elements analysed (Normalised) – all results in weight%

Area	S	Mn	Fe	Total	Comment
1	36.6	60.7	2.7	100.0	MnS particle
2	36.2	59.9	3.9	100.0	
3	37.8	59.4	2.8	100.0	

Figure 62: PN66 nut cross section microstructure

The sulphur content of this PN66 nut was within the specification for ISO898-1 (see Figure 63, below). This may indicate that these nuts are from a different batch/supplier to the other nut fragment found on bolt PN64.



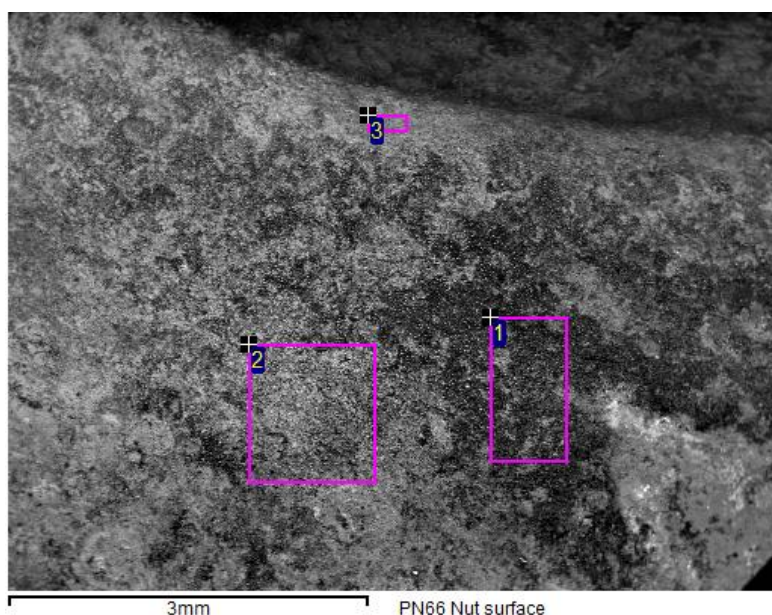
All elements analysed (Normalised) – all results in weight%

Area	S	Mn	Fe	Total
1	0.13	1.69	98.17	100.00
2	0.00	1.67	98.33	100.00
3	0.13	1.82	98.05	100.00
Mean	0.09	1.73	98.18	100.00
Std. deviation	0.08	0.08	0.14	

Figure 63: PN66 SEM cross section and material analysis

Do these show any evidence that they were assembled onto the corroded wall studs at 69.5m?

The PN66 nuts were found on the floor of the trench. They may have been assembled onto the studs at some time but the evidence suggests that these nuts were not assembled onto studs at the time of the fire. Chlorine was present on the inner thread surfaces of the nut that could not have reached this region if the galvanising layer had been in contact with the galvanising layer of the stud thread, Figure 64. The pattern of the thread deposit indicates that this would not have been transferred to the thread if it had been undone after the event. The presence of a fragment of nut on the top stud indicates that the support frame had been correctly assembled and the above finding indicates that the two nuts found on the floor had not been associated with the frame.



Area	C	O	Al	Si	S	Cl	Ca	Mn	Fe	Ni	Zn	Total
1	57.1	16.6	0.9	1.6	0.6	1.9	0.9		8.1	1.5	10.8	100.0
2	35.2	20.8	0.7	0.7	0.4	3.1	0.6	0.7	17.9	1.0	19.0	100.0
3	33.6	21.6	0.3	0.4	0.4	5.9	0.4		5.2		32.3	100.0

Figure 64: PN66 nut surface, SEM image and analysis

The studs show both oxidation/corrosion and arc damage. The nuts show some oxidation and deposition of a carbon/chlorine rich residue, probably associated with the fire. The evidence suggests the nuts were not in place on the studs at the time of the fire.

5. Possible causes of failure of heat shrink transition joint 3-B-0, PN33

5.1 Unlikely causes of failure

There is no evidence to suggest that the cable joint had been subjected to third party mechanical damage.

There is no evidence that the circuit had been carrying excessive load. However, the load pattern on the circuit could be a contributing factor in the failure.

There is no evidence of any arcing activity on the parted bi-metallic connectors. From the oven test at 600°C, the bimetallic weld will separate when the temperature of the connector reaches the levels likely to occur when a major fire occurs in a confined space such as a cable trench. The separation of the bimetallic welds on the PN53 connectors was therefore a result of the fire and not a cause of it.

5.2 Moisture ingress and effect of load changes

It is understood that the XLPE cable length was inserted in 2001. For the last few years the circuit had an open point at one end. The transition cable joints would have received some heat from the other power circuits in the trench but they would not have been heated by current in the 3-B-0 conductors.

It is likely that rain water would have been able to enter the trench through the gaps between the concrete trench covers. The heat shrink transition joint design was potentially susceptible to moisture ingress at the PILC cable end of the joint. The heat shrink outer sleeve coated on the inside with hot melt adhesive was intended to provide protection against moisture ingress. However, it will not prevent moisture from passing along the steel tape armour and along the copper braid earth bonds.

The only point where a seal could potentially be formed between the outer heat shrink sleeve and the lead sheath of the PILC cable was in the gap between the two smaller constant force springs because this gap was not bridged by any copper earth braid. The heating and cooling due to the

short duration application of load to the 3-B-0 circuit could have caused movement of any moisture trapped within the cable crutch.

5.3 Past experience

ERA has examined many failed heat shrink joints onto PILC cables and heat shrink transition joints between XLPE and PILC (mainly belted) cables. The majority of the PILC heat shrink joint failures examined between 2002 and 2014 occurred in the cable crutch area and were attributed to disturbance of the aged paper insulation during the jointing process.

The papers in the aged PILC cable will have lost some of their original mechanical strength and are likely to be susceptible to damage when the cores are flexed during the jointing procedure. Applying the sealing mastic to the cable crutch area could also damage the papers because the mastic sticks to the paper and could cause the paper to tear as the mastic is pushed into the crutch area between the three cores.

On belted cables, the belt papers provide part of the phase to earth insulation. When the belt papers are cut back this part of the phase to earth insulation is lost. In a traditional bitumen filled cable joint the belt cable insulation is replaced by the bitumen and no reduction in phase to earth insulation occurs. The yellow mastic used in Tyco/Raychem joints can provide some additional phase to earth insulation but there can be voids in the mastic depending upon how uniformly it has been applied.

The translucent sealing tubes applied over each core are intended to provide a seal over the paper insulated cores stopping the compound in the papers from drying out and acting as a barrier to stop any moisture reaching the core papers. However it is difficult if not impossible for the jointer to push these sealing tubes completely into the crutch between the three cores. From past examinations there is always a length of PILC cable core which is not covered by a sealing tube and not covered by a lead sheath. This is the susceptible area which is prone to mechanical damage during jointing, prone to drying out of compound, likely to come into contact with any moisture which has entered into the joint and may possibly have a lower phase to earth insulation resistance. From past experience it is at this point that failures tend to occur.

5.4 Position of fault within the 3B0 failed transition joint, PN53

The fault occurred in the PILC cable crutch area. The centre of the arc eroded area was estimated to be 5mm under the translucent core sealing tube. This assumes that the fault propagated from the original site of the breakdown at an equal rate in both directions. The profile of the arc eroded area with a sharp edge almost at right angles to the axis of the cable close to the lead sheath cut back position and a much more rounded profile towards the connectors suggests that the fault did not propagate uniformly in both directions.

It is possible that the initial breakdown was in the area between the end of the translucent sealing tubes and the end of the lead cable sheath and the relatively compact nature of the belted cable with its jute fillers, belt papers, lead sheath and overlying heat shrink boot caused the arc erosion to propagate preferentially into the joint towards the connectors.

5.5 Position of transition joint within the trench

The way that the transition joint was installed within the trench may have been a contributing factor in the failure. It is understood that the PILC cable had been raised to a higher level in the trench so that the transition joint could be made off to the XLPE cable and that as a result the PILC cable end of the joint was not straight. Any bend in the joint at the PILC end could make the cable more prone to moisture ingress and could create voids within the joint at the cable crutch.

5.6 Timing of joint failure

Information on the timing and nature of the faults which occurred in the cable circuits in the trench on the night of the fire are shown in Table 6. This information was provided by CCI.

Table 6: Fault times, position, duration and arc crater volume

Time of Fault	Cable (Circuit)	Fault Position		Fault Type	Fault Duration sec	Fault Current A	Arc Crater Vol. mL
		X-Section	Chainage m				
23:22:00	Remuera K10, 11 kV PILC	3B	73	2 phase 3 phase	0.053 0.508	4,200	27.3
01:21:00	Remuera K10, 11 kV PILC	3B	73	3 phase	0.55	4,200	
02:12:00	Remuera 03, 33 kV XLPE	1A	72.47	Single phase to earth	0.215	16,000	25.8
02:13:00	New Market 3, 33 kV XLPE	1B	73	Single phase to earth	0.131	13,962	-
02:15:00	Carbine Rd 2, 33 kV XLPE	2E	72.8	Single phase to earth	0.364	16,744	16.9
02:17:00	Remuera 02, 33 kV XLPE	1D	72.6	Single phase to earth	0.175	16,500	-
02:23:00	St John 03, 33 kV XLPE	3F	71.13	Single phase B to earth,	1.04	15,916 to 16,338	24.3
			72.8	Single phase R to earth,	0.979	16,932 to 17,463	
02:45:00	McNab K02, 11 kV PILC	3A	67.67	2 phase to earth	0.199	10,370 - 11,190	4.9

02:48:00	Carbine 01, 33 kV OF	2D	68.9	2 phase to earth	0.412	16,000	-
02:48:00	Mt Wellington 02, 33 kV XLPE	4E	66.9	Single phase	0.196	14,500	-
02:48:00	Mt Wellington 01, 33 kV XLPE	5B	-	-	-	-	-
02:48:00	Mt Wellington K05, 11 kV PILC	4D	-	-	-	-	-
02:57:00	Sylvia Park 02, 33 kV XLPE	5D	71.8	Single phase	0.093	14,546	-
03:05:00	McNab K19, 11 kV PILC	2C	67.36	2 phase to earth	0.319	3,980-4,280	1.6
			67.89				3

From the information in Table 3, the incident began at 23:22 as a two phase fault in the Remuera K10, 11 kV PILC cable section which developed into a three phase fault after 0.053 seconds. 0.508 seconds later the circuit tripped out. The fault continued for a further 0.55 seconds when the circuit was re-energised at 01:21. This information supports the conclusion that the original cable fault was in the failed PILC to XLPE transition joint in the 11kV Remuera K10 circuit.

6. Condition of other cable joints

6.1 11kV cast iron joint PN57 3DO, 50m

The cast iron housing was corroded and the bolts securing the two halves of the joint shell together were in some cases almost completely corroded away, Figure 65 and Figure 66. The cable steel tape armour was severely corroded in places. The lead sheath, hessian and papers were missing from the cable on both sides of joint. Papers were still present within the cast iron housing but the lead had melted and re-solidified in the base of the cast iron housing.



Figure 65: Corroded joint shell, PN57



Figure 66: Severely corroded joint shell retaining bolt, PN57



Figure 67: Corroded steel tape armour, PN57

The cable cores within the joint shell were buckled into an S shape within the joint housing and kinked at the armour clamp position at the switch room end of the joint shell, Figure 68. If the ferrules were originally in the centre of the joint, then they had been displaced towards Gavin Street by 85mm.



Figure 68: S shaped profile of cores within joint shell and kink at switchroom end, PN57

There was little if any solder left in the ferrules and one conductor had pulled out of the ferrule by 2.5mm on the switch room side of the joint.



Figure 69: Conductor partly pulled out of ferrule

There was a phase to earth fault in the cable on the Gavin Street side of the joint 280mm away from the end of the joint shell. The phase conductor was eroded over a distance of approximately 10mm. The eroded conductor strands had been displaced outwards through gaps in the armour and there was localised arc erosion on the steel tape armour.



Figure 70: Cable fault position on Gavin St side of joint, PN57



Figure 71: Fault position after removing armour, PN57

There was what appeared to be a second phase to earth fault in another core on the Gavin Street side of the joint 350mm away from the end of the joint shell. The ends of some of the eroded conductor strands had an abraded appearance, Figure 72. The cores may have moved relative to each other and it is therefore possible that there was one phase to phase to earth fault rather than two separate phase to earth faults.



Figure 72: Abraded appearance of conductor strands on Gavin Street side of joint, PN57

6.2 11kV cast iron joint 3BO, PN60

The cast iron joint shell was generally in a good condition but the bolts holding the two halves of the joint shell together and the bolts on the cable armour clamps were eroded, Figure 73. The joint shell

appeared to be full of bitumen but there had been some minor leakage of bitumen from the ends of the joint shell.

The joint shell was heated, drained of bitumen and the two joint shell halves removed. The inner lead sleeve was still intact. It was heated, cut open and drained of bitumen. The core, insulation papers and binders inside the joint all appeared to be in good condition prior to further strip down, Figure 74.



Figure 73: Eroded bolt on cast iron joint shell, PN60



Figure 74: PILC cable joint after removing joint shell, inner lead sleeve and bitumen, PN60

The core papers were damaged where the jointer had bent the cores around a temporary spacer to obtain the correct core profile during the jointing operation but from the visual examination during the strip down there was no evidence of any electrical activity in the core papers at this point.

Some of the core papers had 100% registration. In other words, one layer of tape was wound directly on top of another layer of tape so that the radial butt gap was two tape thicknesses.

There was a hole in the paper tape insulation on core 1 extending from the 8th tape layer through to the conductor. On the surface of one strand of the conductor there was a sharp edged feature which had caused the initial hole in the overlying papers, Figure 75.

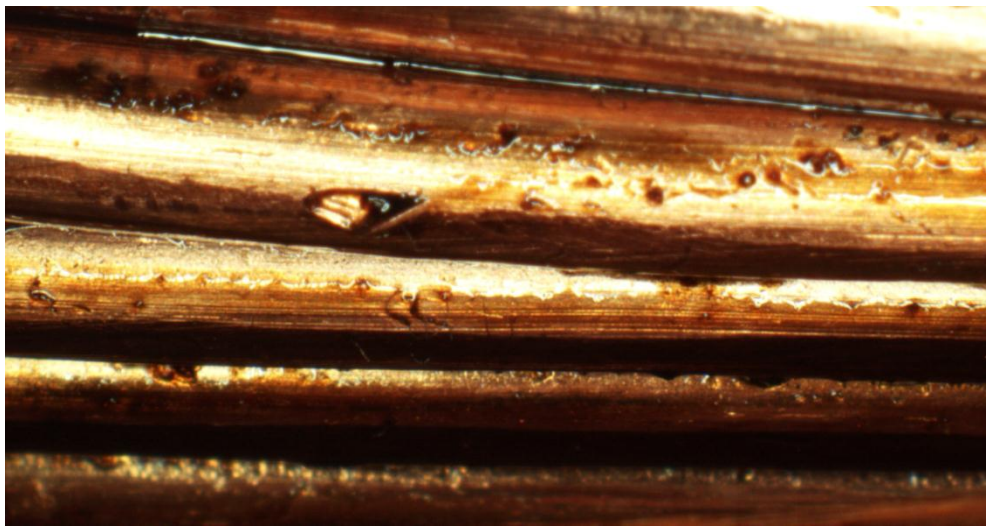


Figure 75: Sharp protrusion from PILC conductor strand, PN60

There was a hole in the paper tape insulation on core 2 extending from the 7th tape layer through to the conductor. At the conductor there was a dark stain on one strand on one corner of the shaped stranded conductor, Figure 76.



Figure 76: Dark stain on conductor beneath hole in core papers, PN60

There was what appeared to be a mixture of bitumen and cable compound in between the conductor strands. There was no evidence of any electrical breakdown in PN60.

6.3 Cast iron joint PN28, 3A0, 71 – 75m

The bolts holding the two halves of the cast iron joint shell were badly corroded, Figure 77.



Figure 77: Corroded bolt on cast iron joint shell, PN28

Lead packing had been used to make a seal between the cast iron box and the lead sheath of the PILC cables. The lead sheath had partly melted outside of the cast iron joint shell due to heat from the fire and the belt insulation papers were degraded where the sheath had melted, Figure 78.



Figure 78: Degraded belt papers, PN28

The core papers had also been degraded, presumably by heat from the fire as there was no evidence of any electrical breakdown activity. The central insulating tapes over the ferrules had been correctly applied and were in relatively good condition. Cloth tape had been applied between the ferrules and the tapered end of the core insulation, Figure 79.



Figure 79: Central taped insulation over ferrule PN28

Most of the solder had melted out of the ferrules. There was a 3mm gap between the Gavin Street end of the ferrule and the cloth tape on core 1 where the conductor had started to pull out of the ferrule, Figure 80.

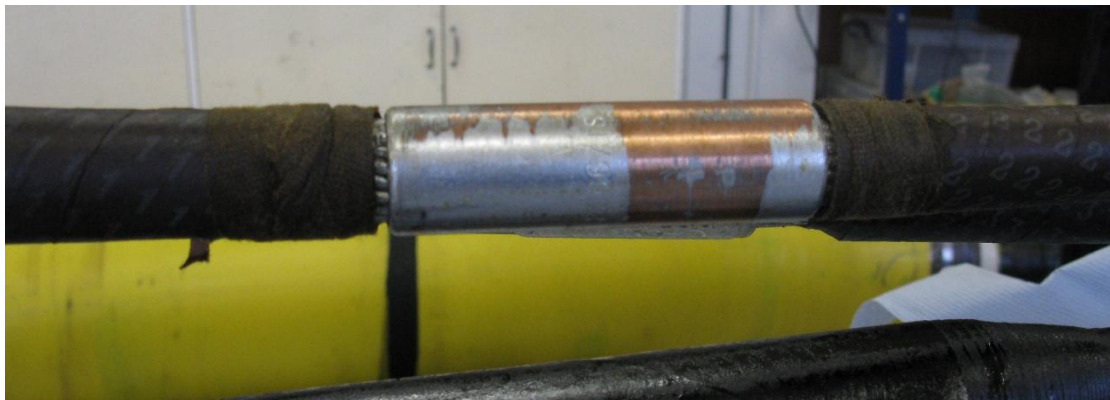


Figure 80: Core 1 ferrule, PN28

There was a dent in the lead sheath, 85mm from the end, at the Gavin Street end of the joint, Figure 81.



Figure 81: Dent in lead sheath, PN28

There was no evidence of any electrical activity or mechanical damage to the belt tapes under the dent in the lead sheath.

The core papers showed signs of localised mechanical damage, creasing and butt gap separation where the temporary spreaders had been fitted during the jointing operation. The lead solder from the ferules had travelled up to 345mm along the conductor strands, Figure 82. The papers had a tendency to split at the extended butt gap positions, Figure 83.



Figure 82: Bend at temporary spreader position and penetration of lead solder, PN28

There were gaps of between 1.5 and 1.8mm between the conductors and the bore of the ferrules, Figure 84.



Figure 83: Split in insulation paper at butt gap position, PN28



Figure 84: Gap visible between conductor and bore of ferrule

6.4 33kV XLPE 800/400mm² transition joint, 1DY, 5m

The hardness of the cable sheath at either end of the joint was measured to be 55 – 65 Shore D.

There was no evidence of any damage to the black outer heat shrink tube. The outer heat-shrink tube and knitmesh copper braid screen were removed to expose the central insulator and earth bond connections, Figure 85.



Figure 85: 33kV XLPE s/c joint after removing outer HS tube and earth screen, PN54

The inside of the outer heat-shrink tube was coated with hot melt adhesive. The portion of the tube sealing onto the smaller diameter cable was 85mm long. The portion of the tube sealing on to the larger diameter cable was 120mm long.

The central insulating tube was 620mm long and was marked "Top layer conducting EB62611 21:50 ECIC 95/42 Raychem". The compression ferrules joining the screen wires from the two cables together were not adequately compressed onto the screen wires. When a cable cutter was used to cut through one of the bunches of screen wires, the ends of the wires fell out of the compression ferrule, Figure 86.



Figure 86: Screen wires fell out of compression ferrule

The central insulation tube and stress control tubes were cut open and removed. A layer of red heat-shrink insulation had been applied over the 400mm² XLPE core to increase its diameter to that of the larger 800mm² cable, Figure 87.



Figure 87: XLPE joint after removing outer heat shrink and stress control tubes PN54

Yellow mastic had been applied over the end of the extruded cores screens, in the gaps between the compression ferrule and the XLPE core insulation and over the compression ferrule. The surface of the yellow mastic was discoloured, particularly at the core screen terminations on both cables. The ends of the XLPE insulation had been tapered, Figure 88.



Figure 88: XLPE core on 400mm² cable and ferrule coated with mastic, PN54

There was no evidence of any electrical activity on the XLPE insulation surface.

6.5 33kV 630/400mm² XLPE insulated transition joint, 03 NWMT YØ 1B-PN59

The 630mm² cable sheath was embossed "General Cable NZX-90 Electric Cable 19/33kV 1C 630mm² AL 2008" and printed "2008 0470 metres -> | <- 0470 metres".

There was no cable sheath on the other end of the joint as the sample had been cut off at the end of the joint, Figure 89. The outer heat shrink tube was cut open and removed. The outer tube was coated with hot melt adhesive on the inside. The ends of the cable sheath had not been abraded.



Figure 89: 400/630mm² XLPE transition joint PN59

The screen wires were connected across the joint with three shear-head bolt connectors, Figure 90.



Figure 90: Screen wire connections across joint, PN59

The central insulator and stress control tubes were cut open and removed. They had all been uniformly shrunk down and there was no evidence of any electrical activity on the core insulation.

Yellow mastic had been applied over the shear-head bolt connector and in the gaps between the core insulation and the ends of the shear-head bolt connector. The gaps above the ends of the shear-head bolts had been filled with a cream coloured putty, Figure 91.



Figure 91: Shear head bolt connector, PN59

6.6 XLPE single core transition joint, Remuera No. 2, 1DZ, PN55

The Raychem WCSM 160/50 outer tube was uniformly shrunk down onto the joint with hot melt adhesive visible at either end, Figure 92. The WCSM outer tube and the semi-conducting CNTM stress control tubes were cut open and removed. The ends of the cable sheaths had not been abraded.



Figure 92: Hot melt adhesive visible at end of WCSM outer tubing, PN55

The screen wires had been connected using compression ferrules. The ferrules had been properly compressed onto the screen wires.

The central insulator and underlying black heat shrink tube were cut open and removed. Red heat shrink tubing, Raychem EB10661-05 100/40, had been applied over the smaller diameter cable to

build up the diameter. There was a thin layer of oil over the red heat shrink tubing. Yellow mastic had been applied over the ferrule and screen terminations. The yellow mastic was discoloured at the ends of the ferrule and at the screen terminations, Figure 93.



Figure 93: Yellow mastic applied over ferrule and screen terminations, PN55

The XLPE insulation was close to the original colour on the 400mm² side of the joint but darker on the 800mm² side, Figure 94.



Figure 94: XLPE insulation and compression ferrule, PN55

The distance from the screen cut back position to the ferrule was 226mm on the 400mm² side of the joint and 145mm on the 800mm² side of the joint.

6.7 XLPE transition joint Newmarket 03 Red Phase, PN58

The 960mm long WCSM outer heat shrink tube was uniformly shrunk down onto the joint. The outer heat shrink tube and knitmesh braid was cut open and removed from the joint, Figure 95.



Figure 95: XLPE transition joint after removing outer WCSM tube, PM58

The outer heat shrink tube was coated on the inside with hot melt adhesive. The ends of the cable sheaths had not been abraded, Figure 96.



Figure 96: End of cable sheath and remains of hot melt adhesive, PN58

The screen wires were joined together across the joint with compression ferrules. The central insulator was cut open and removed. There was no evidence of any electrical activity within the joint.

There was a layer of stress control tube over the phase conductor compression ferrule, Figure 97.



Figure 97: Stress control tube over phase conductor ferrule and screen wires connection, PN58

The stress control tube was cut open and removed. Yellow mastic had been applied at the screen terminations, between the ferrule and the ends of the XLPE insulation, and over the compression ferrule.

The XLPE insulation was close to the original colour on the 400mm² side of the joint but darker on the 800mm² side, Figure 98.



Figure 98: XLPE insulation and compression ferrule, PN58

The distance from the screen cut back position to the ferrule was 226mm on the 400mm² side of the joint and 145mm on the 800mm² side of the joint.

6.7.1 33kV XLPE 800/400mm² transition joint, PN 56, 1AX, 5m

The PN56 transition joint was examined by Brian Gregory from Cable Consulting International assisted by a technician from Edif ERA. The following account of the examination was written by Brian Gregory:

The larger cable was embossed "Olex 800mm² Al XLPE 1999". The smaller cable had been cut short and the legible part of the embossing read "Electric Cable 19/33 kV"; it was identified to be 400 mm² aluminium conductor cable supplied by General Cable, NZ.

The hardness of the cable sheath at the 400 mm² end was 61 Shore D and on the 800mm² end 66 Shore D.

There was no evidence of any damage to the protective outer black heat shrink sleeve. The heat shrink sleeve and knit-mesh copper braid screen were removed to expose the two earth bond connections and the central insulation package, Figure 99.



Figure 99: 33kV XLPE s/c joint after removing outer HS tube and earth screen, PN56

The inside of the outer heat-shrink tube was well coated with hot melt adhesive, which adhered to the knitmesh screen, but not to the insulation package sleeve below it. The sleeve was well adhered onto the 400 mm² cable sheath over a 140mm length and onto 800 mm² length over a 150mm length.

The central insulation package sleeve, a dual layer semi-con and elastomeric insulating tube, was 635mm long and was marked "Top layer conducts EB62611 21:12 ECIC 95/42 Raychem". The sleeve was cut off. The outer 3 mm thick layer was confirmed to be conducting, having a low resistance of 20 k Ω , and the 8.4 mm thick pink EPR insulation confirmed to have a high resistance of >200 G Ω .

The cable screen wires were divided into two bunches and each connected to the opposite cable by indent ferrules. The ferrules had deep indents and had been compressed to firmly grip the screen wires. The resistance across the ferrule was satisfactory at 15.3 $\mu\Omega$.

The ferrule length appeared to have been too short to accommodate the indent widths. On one ferrule, Figure 100, two of the indents were ineffective: one was compressed at the centre of the ferrule and another overlapped the end of the ferrule.



Figure 100: Ferrule connecting cable screen wires across the joint PN 56

The underlying heat shrink sleeve was of length 635 mm, black and marked "Raychem JSCR 76/33 STRESS CONTROL EB 42431-02". The sleeve was confirmed to have a high resistance of $>200G\Omega$ at 1000V.

The stress control sleeve was cut open and removed. A thick layer of silicone oil was present below it. Figure 101 shows the sleeve partly pulled back off the ferrule. The conductor connector was covered with well adhered yellow void filling mastic in which a 10-11 mm void was present. A longitudinal ridge of aluminium was protruding through the yellow mastic in close proximity to the void. The ridge had been formed by the pinching of the aluminium ferrule between the hexagonal shaped compression dies. It is good practice to reduce a pronounced ridge by rotating the dies and repressing them, or by filing the protrusion off.

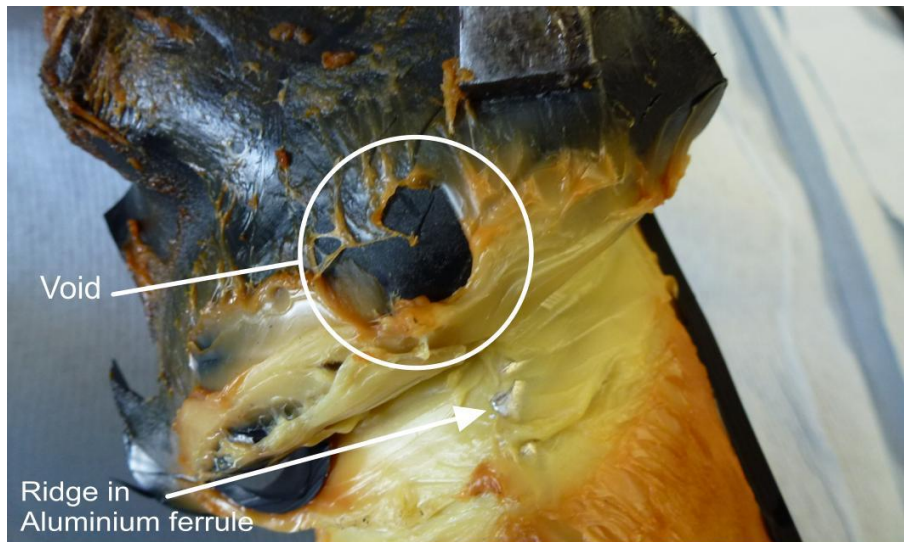


Figure 101: yellow mastic showing void and ridge of aluminium ferrule PN 56

The inner surface of the stress control sleeve was marked with a mottled matt surface at its interface with the void and was possibly indicative of partial discharge activity. This surface was later examined; no evidence of partial discharge erosion was found on the sleeve. The void and the aluminium ridge are undesirable features that may reduce electrical performance.

Two red heat shrink insulating sleeves 208 mm long had been applied over the 400mm² XLPE core to increase the insulation diameter to that of the larger 800mm² cable. One sleeve was marked: Raychem 65/25 EB11662-10.

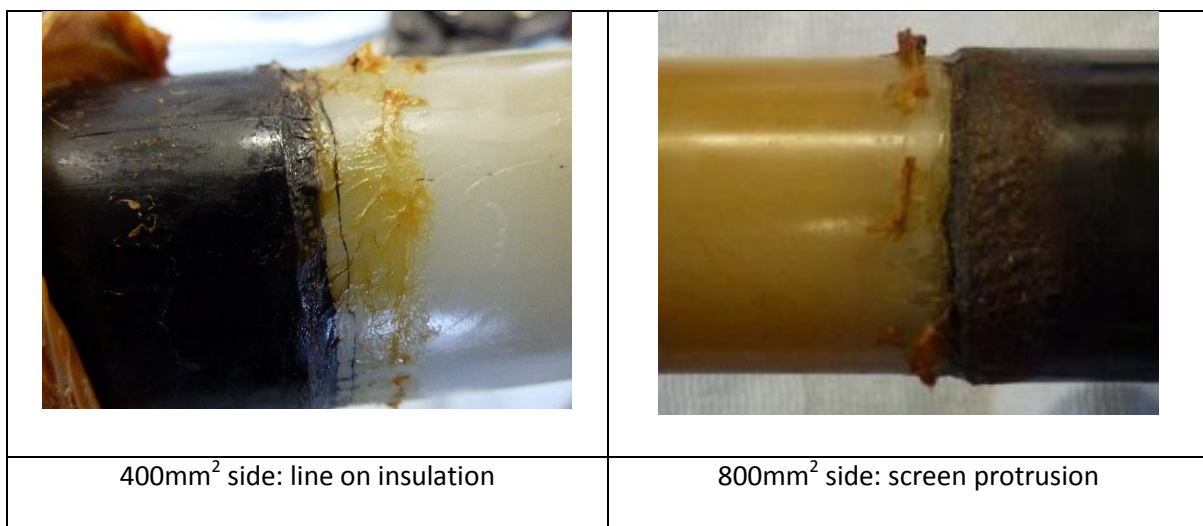


Figure 102: Screen termination features PN 56

The red sleeves were removed from the 400mm² side. The local covering of yellow void filling mastic was removed to reveal the termination of the cable's extruded core screen, Figure 102 left hand side. The screen had been chamfered to approximately 45°. A circumferential black line was present

on the XLPE core insulation a distance of 1.5 mm from the screen termination. The line was thought to be the remnants of the jointer's preparation of the screen cut.

The void filling mastic applied over the screen termination on the 800mm² cable side had discoloured from yellow to both dark red and to black, indicative of ageing and chemical activity between the materials present. The yellow mastic was removed from the 800mm² cable side, Figure 102 right hand side, to reveal a small stress raising protrusion present on the edge of the core screen termination where it had not been uniformly removed.

The screen terminations showed evidence of low jointing standards. Good practice is to remove screen protrusions and remnants of the semiconducting screen as these form electrical stress raisers.

A marked difference in colour of the two cable XLPE insulations was apparent, Figure 102, that was attributed to difference in the types of the anti-oxidants. The colour of the insulation on the 400mm² side was white-light grey and on the 800mm² side was a darker light-brown colour. There was no evidence of any electrical activity on the XLPE insulation surfaces.

The yellow mastic was removed from the ferrule and found to be well adhered, Figure 103. The ferrule was asymmetrically positioned in length on the conductors having a small gap to the insulation cut on the 400 mm² side and a larger 12mm wide gap on the 800 mm² side, Figure 103. Wide gaps are undesirable as they risk void formation and mechanical instability.



Figure 103: Compression transition ferrule PN56

A lateral bend of 4mm offset was present over the ferrule length. A possible cause of bending is the use of a two-part compression die in a press having a single hydraulic ram. Curvature is undesirable as it increases the risk of void formation at the interface between the joint insulation and the cable XLPE insulation.

7. Conclusions

- Based on the timings of the cable faults that were recorded, the position of the fault, its appearance and from past experience, the PILC/XLPE transition joint fault in the 11kV Remuera K10 circuit was the original fault and not a result of the fire.
- From the profile of the eroded area, the fault position and from previous experience, the PILC/XLPE transition joint fault started in the PILC cable crutch and the arc propagated preferentially away from the cable crutch towards the phase connectors.
- A black feature/stain indicative of deterioration or possibly incipient electrical distress was present on the PILC core paper tape insulation of the unfailed PILC to XLPE transition joint below the lead sheath and in the vicinity of the lead cut. Components of the yellow void filling mastic were present in the feature.
- From Edif ERA's previous experience of examining failed PILC cable joints, the PILC cable crutch is a weak area where failures are likely to occur in heat shrink joints on aged belted PILC cables.
- The bimetallic ferrules in the PILC to XLPE transition joints were found to have been sound. The parting of the bimetallic interface was found to be a consequence of the fire. The compression ferrules were found to have been sound.
- A portion of nut was found to be present on the top wall stud of the collapsed cable support frame, thus confirming that the frame had been assembled correctly. The evidence suggests the nuts found on the floor of the cable trench at 69.5m, the position of the collapsed cable support, were not in place on the studs at the time of the fire. The evidence indicates that the nuts had not been associated with the frame.
- The PILC cables in the cable trench had severely corroded steel tape armour but this would not have affected the life of the cables as long as the cables were not subjected to mechanical impacts.
- The PILC cable cast iron joint shells were corroded and had slight bitumen leaks but this would not have affected the life of the cast iron joints because they have an inner bitumen filled lead sleeve.
- There was a sharp point on one strand of the PILC cable in the PN60 cast iron cable joint. This could have developed into a breakdown fault in perhaps 5 to 10 years (a very rough estimate).
- The five XLPE straight joints examined were generally found to be in sound condition. In one joint one of the two compression ferrules connecting the cable earth return conductors had not satisfactorily gripped the conductor wires.
- There were no other incipient faults in any of the joints sent to ERA for examination.

8. References

1. Stubbs J, Analysis of samples taken from cable trench at Penrose Substation, Edif ERA Report 205-0027, Edif ERA, Leatherhead, 2015.
2. www.mace.manchester.ac.uk/project/research/structures/strcfire/DataBase/References/Reinstatement_Fire_Damaged_Steel
3. www.galvanizeit.org/hot-dip-galvanizing/how-long-does-hdg-last/in-extreme-temperatures
4. www.galvanizeit.org/education-and-resources/resources/technical-faq-dr-galv/galvanized-steels-performance-in-extreme-temperatures